The University of Alberta
Printing Department
Edmonton, Alberta

T H E U N I V E R S I T Y O F A L B E R T A

RELEASE FORM

NAME OF AUTHOR ..... JAMES HODGKINSON .....

TITLE OF THESIS ..... NMR Line Broadening and Chemical Shift Study of Iron(III) and Iron(III) Porphyrin Systems .....

DEGREE FOR WHICH THESIS WAS PRESENTED ..... M.Sc. .....

YEAR THIS DEGREE GRANTED ..... 1975 .....

DATED 18 December

THE UNIVERSITY OF ALBERTA

NMR LINE BROADENING AND CHEMICAL SHIFT STUDY OF IRON(III) AND IRON(III) PORPHYRIN SYSTEMS

BY

© JAMES HODGKINSON

A THESIS

SUBMITTED TO THE FACULTY OF GRADUATE STUDIES AND RESEARCH

IN PARTIAL FULFILMENT OF THE REQUIREMENTS FOR THE DEGREE

OF

MASTER OF SCIENCE

DEPARTMENT OF CHEMISTRY

EDMONTON, ALBERTA

SPRING, 1975

THE UNIVERSITY OF ALBERTA

FACULTY OF GRADUATE STUDIES AND RESEARCH

The undersigned certify that they have read, and recommend to the Faculty of Graduate Studies and Research for acceptance, a thesis entitled

"NMR LINE BROADENING AND CHEMICAL SHIFT STUDY OF IRON(III) AND IRON(III) PORPHYRIN SYSTEMS"

submitted by JAMES HODGKINSON in partial fulfilment of the requirements for the degree of Master of Science.

December 6, 1974

Date

TO ROSEANN

A B S T R A C T

The solvent exchange reactions of iron(III) perchlorate in N,N-dimethylformamide (DMF) and of α,β,γ,δ-tetraphenylporphineiron(III) perchlorate and porphineiron(III) perchlorate in DMF and methanol were investigated using nmr line broadening and chemical shift methods. Chemical exchange controlled line broadening of the bulk solvent proton resonance was observed in all the solutions studied.

The solvent exchange rates from the iron(III) porphyrins are about 10^5 times faster than from $Fe(DMF)_6^{3+}$. This large rate enhancement has been observed in cobalt(III) systems as well. The cobalt(III) and iron(III) porphyrins differ in that the iron atom is above the plane of the porphyrin ligand while cobalt is in the plane.

It is concluded that this structural difference is not the source of lability in the porphyrins. A comparison of the iron(III) porphine and tetraphenylporphine systems indicates that the sigma donor ability of the porphyrin ligand is not a major contributor to the large exchange rates. It is suggested that pi bonding in the transition state may be the source of the lability of the porphyrins.

The very negative activation entropy for $Fe(DMF)_6^{3+}$ - DMF exchange is some evidence that the exchange mechanism is associative.

Two equations correlating the activation enthalpy of solvent exchange and solvent basicity are discussed. Good two-parameter correlation is found for a number of metal ion-solvent systems.

A C K N O W L E D G E M E N T S

I wish to express my gratitude to Dr. Robert B. Jordan for his help and patience during this work.

I also wish to gratefully thank Mrs. Mary Waters for the excellent preparation of this manuscript.

Financial assistance from the University of Alberta is gratefully acknowledged.

TABLE OF CONTENTS

Page

L I S T O F T A B L E S

L I S T O F F I G U R E S

CHAPTER I INTRODUCTION

1. General Comments

The work of this thesis resulted from a desire to study how the solvent exchange rate is affected in going from hexasolvated metal ions to metalloporphyrin complexes.[1,2,3] The study of iron(III) porphyrin compounds was undertaken because of their relevance as biological models. The heme structure of hemoproteins has received much attention during the last decade, and has been examined by a variety of physical techniques, including magnetic, optical, EPR, Mössbauer [4] and NMR spectroscopy [5]. These studies provide a wealth of general physical and chemical data which could aid in the present work.[4,5,6]

The nature of the two porphyrin ligands chosen was determined from their relative donicity.[7] The two porphyrins studied here are at opposite ends of a relative donicity scale, such that any differences in exchange rate due to the nature of the porphyrin group should be maximized.

The solvent exchange process involves the displacement of a solvent molecule bound to the paramagnetic ion, iron(III) in this case, by a solvent molecule from the bulk solvent. In general such a reaction is termed a substitution reaction.[8,9]

These reactions are typified by the following equations

$$S_5M\text{-}S^{m+} + S^* \underset{k_{-1}}{\overset{k_1}{\rightleftharpoons}} S_5M\text{-}S^{*m+} + S \qquad (1)$$

and

$$L_xM\text{-}S^{m+} + S^* \underset{k_{-1}}{\overset{k_1}{\rightleftharpoons}} L_xM\text{-}S^{*m+} + S \qquad (2)$$

where S and S^* are initially coordinated and free solvent molecules, respectively, and L_x represents any non-exchanging ligand(s). For example if M = Fe(III) and S = N,N-dimethylformamide (DMF), solvent exchange from octahedral $Fe(DMF)_6^{3+}$ to solvent DMF is represented by equation 1. In equation 2, if L_x = α,β,γ,δ-tetraphenylporphine, (TPP); M = Fe(III), and S = methanol, (MeOH), solvent exchange from the porphyrin $FeTPP(MeOH)^+$ to solvent methanol is represented.

Since no net chemical change occurs it is impossible to study solvent exchange processes by classical kinetic methods, but such reactions may be studied by the nmr line broadening method. The latter has been applied to a variety of systems, spanning an enormous range of rate constants.[10,11-14] For example, Stengle and Langford [10] cite solvent exchange rate constants (at 25°C) ranging from 0.5 to 8 x 10^9 sec^{-1} measured using the nmr method.

The rate at which these processes occur may be characterised by the lifetime (τ_M) of the solvent molecule(s) in the first coordination sphere of the metal ion.

This lifetime is given by the general definition

$$\tau_M^{-1} = \frac{\text{Rate of solvent removal from metal site}}{\text{Concentration of solvent in metal sites}} \quad (3)$$

If the rate of exchange is a first order process

$$\text{Rate} = k_1[M]$$

$$\text{Concentration} = n[M]$$

(where n is the number of solvent molecules in the first coordination sphere), then,

$$\frac{1}{\tau_M} = \frac{k_1[M]}{n[M]} = \frac{k_1}{n} \quad (4)$$

If the rate is a second order process

$$\text{Rate} = k_2[M][S],$$

and therefore,

$$\frac{1}{\tau_M} = \frac{k_2[S]}{n} \quad . \quad (5)$$

Normally the nmr method is unable to distinguish between equations (4) and (5) since [S], the concentration of the solvent, remains constant. However, the use of mixed solvents, if one solvent is non-coordinating (nitromethane or dichloromethane) can distinguish between the unimolecular and bimolecular exchange mechanism. Frankel has found that ligand exchange parameters for Ni(II) in DMF and dimethylsulfoxide are independent of the composition of the

mixed solvent.[15,16] Therefore the solvent exchange in these systems is a unimolecular process and probably proceeds by a dissociative type mechanism (see below, equation 7).

The nmr method can yield values for the activation enthalpy ($\Delta H^{\ddagger}$) and activation entropy ($\Delta S^{\ddagger}$) for the exchange reactions. A comparison of these results from various systems can be of value in revealing the intimate mechanism of the exchange reaction.

Some success has been achieved in correlating $\Delta H^{\ddagger}$ values to theoretical crystal field activation energies.[8,10] Specifically, $\Delta H^{\ddagger}$ values for solvent exchange by octahedral + 2 metal ions can be qualitatively correlated with crystal field activation energies calculated for five coordinate intermediates involved in a dissociative mechanism,

$$MX_n \underset{+X}{\overset{-X}{\rightleftharpoons}} [MX_{n-1}] \underset{-Y}{\overset{+Y}{\rightleftharpoons}} MX_{n-1}Y \quad . \qquad (7)$$

$\Delta S^{\ddagger}$ values may be used to infer association or dissociation in proceeding to a transition state. In particular, a large negative $\Delta S^{\ddagger}$ may be indicative of an associative mechanism [17-21],

$$MX_n \underset{-Y}{\overset{+Y}{\rightleftharpoons}} [MX_nY] \underset{+X}{\overset{-X}{\rightleftharpoons}} MX_{n-1}Y \quad . \qquad (8)$$

A third mechanism is possible, where no intermediates of reduced or increased coordination number can be detected,

the interchange mechanism [9],

$$MX_n \ldots Y \longrightarrow MX_{n-1}Y \ldots X \qquad (9)$$

This mechanism can be further categorised as dissociative (I_d) or associative (I_a), depending on whether bond breaking or making is more important in reaching the transition state.

In some cases no direct information on the solvent exchange process may be obtained because the reaction is either too fast or too slow for the nmr method. It is usually possible to decide between these two alternatives from the magnitude of the effect of the metal ion on the nmr spectrum. Then one can at least determine qualitatively whether the system is very labile, and exchange is fast, or very inert and exchange is slow.

Structural studies of metalloporphyrin chemistry have established the five-coordinate, square pyramidal structure for high spin iron(III) porphyrin complexes.[5,7,22-25] The X-ray studies on FeTPPCl [26], α-chlorohemin [27] and methoxy-iron(III)mesoporphyrin(IX)dimethylester [28] (MeOFeDMMesopor) have indicated the following structure:

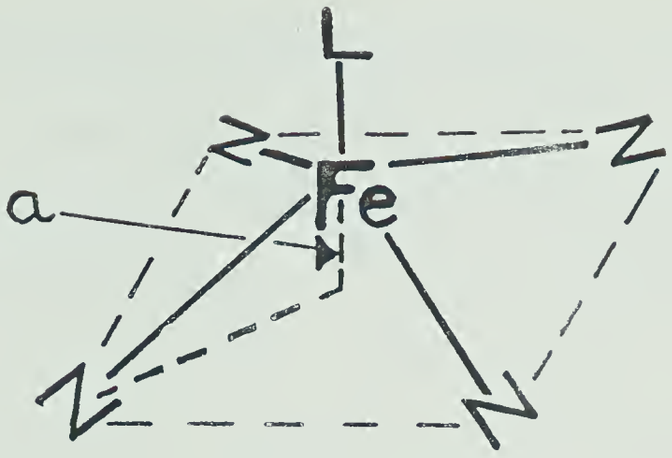

where a is the distance the high spin Fe(III) is displaced above the plane of the four coordinating nitrogens. In FeTPPCl, a = 0.383 Å, in α-chlorohemin, a = 0.475 Å and in MeOFeDMMesopor a = 0.455 Å.

These observations are consistent with the theoretical calculations of Gouterman et al which stress that an out-of-plane displacement of the iron(III) atom is required for stability in high spin iron(III) porphyrins.[29-32]

It will be assumed throughout this thesis that in methanol and N,N-dimethylformamide the iron(III) porphyrin retains a coordination number of five by binding one solvent molecule when the initial chloride ligand is removed.

Magnetic susceptibility measurements have shown that in porphyrin complexes of the type LFe(III)P (where L is a monovalent anion; halide, SCN^-, etc.,) iron is high-spin requiring the assignment of a $^6S_{5/2}$ ground state.[6] Effective magnetic moments for these complexes are usually about 5.9 BM at room temperature.[6,33-35]

Far infrared techniques have been used to directly

measure the zero-field splittings present in these complexes.[36,37] In addition EPR [38] and NMR [39] spin-lattice relaxation measurements and magnetic susceptibility temperature dependence studies [33,34] have yielded indirectly zero-field splitting values. These results indicate a dependence of zero-field splitting on the nature of the axial ligand L, and values in the range 10 - 40 cm^{-1} have been reported for a variety of iron(III) porphyrins.

2. NMR Theory for Solvent Exchange

Figure 1 illustrates the derivation of observed line broadening and shift data from experimental nmr spectra. Spectrum (a) is that of pure solvent, (b) that of the solvent in the presence of a paramagnetic species, i.s., the internal standard (reference compound) and $h_{1/2}$, half the peak height. The following observables are defined in frequency units (Hz),

$$\Delta\nu_{obsd} = C\text{-}D \text{ Hz} \tag{10}$$

$$\Delta\nu_{sol} = E\text{-}F \text{ Hz} \tag{11}$$

$$\nu_{obsd} = B\text{-}S \text{ Hz} \tag{12}$$

$$\nu_{sol} = A\text{-}S \text{ Hz} \tag{13}$$

The solvent shift can be further expressed in rad. sec^{-1} units,

$$\Delta\omega_{obsd} = 2\pi(\nu_{obsd} - \nu_{sol}) \tag{14}$$

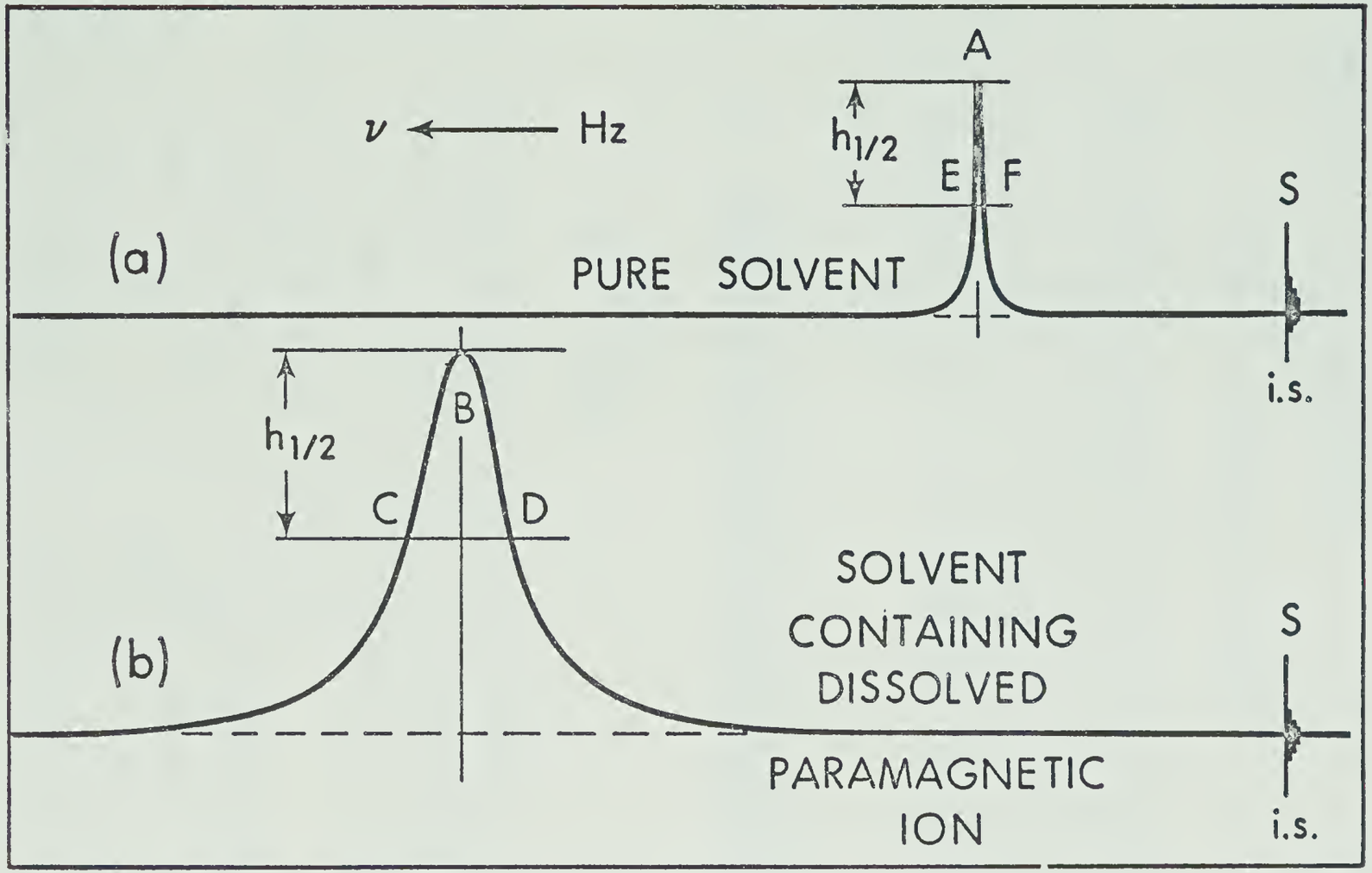

FIGURE 1. Analysis of nmr spectra for shift and line broadening data

For a Lorentzian absorption signal [40], the increase in transverse relaxation rate of the observed nucleus due to the paramagnetic ion is given by,

$$(T_{2P})^{-1} = \pi(\Delta\nu_{obsd} - \Delta\nu_{sol}) \qquad (15)$$

This quantity is generally dependent on the concentration of the dissolved paramagnetic species and the temperature of the solution. Concentration effects are accounted for by normalising the line broadening and shift, by dividing each by P_M, where

$$P_M = \frac{\text{Number of coordinated solvent molecules}}{\text{Number of non-coordinated solvent molecules}}$$

$$= \frac{n[M]}{[S]_o - n[M]} \qquad (16)$$

Here, $[S]_o$ represents the total molal solvent concentration, [M] is the molal concentration of the paramagnetic species and n is the number of solvent molecules in the first coordination sphere of the metal ion.

In general, $(T_{2P})^{-1}$ and $\Delta\omega_{obsd}$ are directly proportional to P_M, hence $(T_{2P}P_M)^{-1}$ and $\Delta\omega_{obsd}/P_M$ should be constant (within experimental error) for samples containing different amounts of paramagnetic ions, when comparisons are made at the same temperature. Indeed such a consistency of values is a test of the technique used in preparing solutions of accurate concentration.

The effect of temperature on $(T_{2P}P_M)^{-1}$ and $\Delta\omega_{obsd}/P_M$ is more complex and Chapter III will be concerned with the interpretation of the variation of $(T_{2P}P_M)^{-1}$ and $\Delta\omega_{obsd}/P_M$ with temperature in terms of parameters of kinetic and physical significance.

Understanding of the paramagnetic ion induced line broadening and shift has come about principally through the work of Swift and Connick [41,42], who first solved the Bloch equations, as modified by McConnell [43], for systems undergoing exchange between two sites, with one of the sites in large stoichiometric excess. These conditions apply in the present case since the solvent is in great excess. Swift and Connick showed that [41]

$$(T_{2P}P_M)^{-1} = \frac{1}{\tau_M}\left(\frac{(T_{2M})^{-2} + (\tau_M T_{2M})^{-1} + \Delta\omega_M{}^2}{\left(\frac{1}{T_{2M}} + \frac{1}{\tau_M}\right)^2 + \Delta\omega_M{}^2}\right) + T_{2O}{}^{-1} \qquad (17)$$

and

$$-\frac{\Delta\omega_{obsd}}{P_M} = \frac{\Delta\omega_M}{\left(\frac{\tau_M}{T_{2M}} + 1\right)^2 + (\tau_M\Delta\omega_M)^2} \qquad (18)$$

for solvent exchange between two sites. The terms in these equations will be discussed now.

(i) τ_M: This is the residence time (in seconds) of a

solvent molecule attached to the paramagnetic site as defined in equations 4 and 5. Variation of τ_M with temperature is given by the transition state theory of reaction rates,

$$\tau_M = (kT/h)^{-1} \exp (\Delta H^{\ddagger}/RT - \Delta S^{\ddagger}/R) \qquad (19)$$

where k is Boltzmann's constant, h is Planck's constant, T is the absolute temperature, R is the gas constant, $\Delta H^{\ddagger}$ and $\Delta S^{\ddagger}$ are the enthalpy and entropy of activation respectively.

(ii) $\Delta\omega_M$: This is the chemical shift of the coordinated solvent nuclei due to interaction with the unpaired electrons of the metal ion complex.

It has been shown by Bloembergen that the Fermi contact shift can be expressed as [44]

$$\Delta\omega_M = -(\frac{A}{\hbar}) \frac{\omega_o \mu_{eff}^{\beta} \sqrt{S(S+1)}}{3kT\gamma_I} \qquad (20)$$

$$= -\frac{C_\omega}{T} \qquad (21)$$

Thus, C_ω is a function of the operating frequency of the NMR spectrometer (ω_o, rad sec^{-1}), the spin quantum number of the paramagnetic ion (S), the effective magnetic moment μ_{eff} of the complex and the electron-nucleus hyperfine coupling constant ($A/\hbar$, rad sec^{-1}). The constants are the Bohr magneton, β, the nuclear magnetogyric ratio of the

nucleus, γ_I, and Boltzmann's constant, k. The value of $\Delta\omega_M$ can be obtained from $\Delta\omega_{obsd}$, through equation 18.

(iii) T_{2M}: This is the relaxation time of the solvent nuclei bound to the metal ion. Solomon and Bloembergen [45, 46] have derived theoretical expressions for T_{2M} in terms of fundamental atomic and statistical properties of the metal ion-solvent system.

$$(T_{2M})^{-1} = \left\langle \frac{1}{r_i^6} \right\rangle \frac{\gamma_I^2 g^2 \beta^2 S(S+1)}{15} f_D(\tau_D) + \frac{1}{3}(A/\hbar)^2 S(S+1) f_e(\tau_e) \quad . \tag{22}$$

The first term in equation 22 is due to the dipole-dipole through space interaction between the solvent nuclei and metal ion electron(s). The second term arises from a hyperfine interaction (Fermi contact) due to the finite probability of transferring electron spin density through chemical bonds to the solvent nucleus.

In equation 22, r_i is the length of the vector connecting the nucleus and metal ion and g is the electronic g factor. The correlation time functions $f_D(\tau_D)$ and $f_e(\tau_e)$ are defined as follows [47],

$$f_D(\tau_D) = 7\tau_{D1} + \frac{13\tau_{D2}}{1 + \omega_S^2 \tau_{D2}^2} \tag{23}$$

and

$$f_e(\tau_e) = \tau_{e1} + \frac{\tau_{e2}}{1 + \omega_S^2 \tau_{e2}^2} \qquad (24)$$

when $\omega_I << \omega_S$, $\omega_I^2 \tau_e^2 << 1$ and $\omega_I^2 \tau_D^2 << 1$. Here, ω_I and ω_S are the Larmor frequencies for the resonating nucleus and electron(s) respectively. The correlation times in equations 23 and 24 are given by

$$\tau_{D1}^{-1} = \tau_{e1}^{-1} + \tau_r^{-1} = (T_{1e}^{-1} + \tau_M^{-1}) + \tau_r^{-1} \qquad (25)$$

and

$$\tau_{D2}^{-1} = \tau_{e2}^{-1} + \tau_r^{-1} = (T_{2e}^{-1} + \tau_M^{-1}) + \tau_r^{-1} \qquad (26)$$

where τ_r is the rotational correlation time of the paramagnetic complex in the solvent, and T_{1e} and T_{2e} are the longitudinal and transverse electron spin relaxation times, respectively.

According to McLachlan [48], average values of T_{1e} and T_{2e} are given by

$$\left\langle 1/T_{1e} \right\rangle = \frac{1}{50}\Delta^2 \left\{ 4S(S+1) - 3 \right\} [J_1 + 4J_2] \qquad (27)$$

and

$$\left\langle 1/T_{2e} \right\rangle = \frac{1}{100}\Delta^2 \left\{ 4S(S+1) - 3 \right\} [3J_0 + 5J_1 + 2J_2] \qquad (28)$$

In these equations Δ^2 is the trace of the square of the zero field splitting (Z.F.S.) tensor,

$$\Delta^2 = \frac{2}{3} D^2 + 2E^2 \quad , \qquad (29)$$

since the electronic relaxation rate for S = 5/2 ions is generally assumed to be controlled by the modulation of the quadratic Z.F.S. interaction [49], with Hamiltonian

$$\mathcal{H}_{ZFS} = D[S_z^2 - \tfrac{1}{3}S(S+1)] + E(S_x^2 - S_y^2)$$

where (x,y,z) is the molecular axis system, D and E are coefficients which describe the effects of axial and rhombic ligand fields, respectively.

The power spectrum terms in equations 27 and 28, J_n, are given by [48]

$$J_n = \frac{2\tau_c}{1 + n^2\omega^2\tau_c^2} \qquad (30)$$

Here, $\tau_c = \tau_r$, the rotational or tumbling correlation time for the metal ion complex.

In most circumstances, equation 22 can be approximated to the form

$$(T_{2M})^{-1} = C\tau_r \qquad (31)$$

$$= C_M \exp(E_M/RT) \qquad (32)$$

where the temperature dependence of the rotational correlation time τ_r has been assumed to be

$$\tau_r = \tau_r^{o} \exp(E_r/RT) \qquad (33)$$

The parameter E_M in equation 32 is an effective activation

energy and C_M a constant, with sec^{-1} units.

(iv) T_{2O}: The outer-sphere contribution to line broadening (T_{2O}^{-1}) due to dipole-dipole interactions between unpaired electrons of the metal ion and molecules outside the first coordination sphere, has been shown to be [50]

$$T_{2P}^{-1} = \frac{4}{45}\pi \frac{(10^{-3}\rho N[M])S(S+1)\gamma_I^2 g^2 \beta^2 f_D(\tau_D)}{d_o^3} \qquad (34)$$

In this equation, d_o is the outer-sphere interaction distance in cm, ρ is the solvent density and N, Avagadro's number.

It is convenient to rewrite equation 34 eliminating the concentration term [M], since in the present work the observed line broadenings (T_{2P}^{-1}) are normalised to $P_M = 1$. Hence,

$$(T_{2O})^{-1} = \frac{4.14 \times 10^{13} S(S+1)\rho f_D(\tau_D)}{r_o^3} \cdot \frac{[S]}{n} \qquad (35)$$

where r_o is the outer-sphere interaction distance in $\mathring{A}$ units, numerical substitutions have been made and $(T_{2O})^{-1}$ represents $(T_{2P})^{-1}$ normalised to $P_M = 1$.

$(T_{2O})^{-1}$ may be described by

$$(T_{2O})^{-1} = C_O \exp(E_O/RT) \qquad (36)$$

where C_O is a constant in sec^{-1}, and E_O an activation energy

term dependent on the solvent.

To sum up, the temperature dependence of line broadening $(T_{2P}P_M)^{-1}$ and chemical shift $(\Delta\omega_{obsd}/P_M)$ depends on the following functions and parameters:

(i) τ_M ----- $\Delta H^{\ddagger}$ and $\Delta S^{\ddagger}$

(ii) $\Delta\omega_M$ ---- C_ω

(iii) T_{2M} ---- E_M and C_M

(iv) T_{2O} ---- E_O and C_O

The seven parameters listed above on the right may be inserted into the Swift and Connick equations (equations 17 and 18), replacing the above functions on the left with temperature dependent functions.

The resulting expression may then be used in conjunction with a suitable non-linear least-squares computer program to provide the best-fit of the observed data to the equation, using the seven parameters as adjustable, or fixed parameters. This process will be discussed for each case, but usually involves obtaining agreement between linewidth and shift data by fixing some parameters whilst allowing others to vary, and observing the sensitivity of the numerical fit to such variations. The object is to obtain values for $\Delta H^{\ddagger}$, $\Delta S^{\ddagger}$, C_ω, E_M, C_M, C_O and E_O consistent with all of the observed data.

CHAPTER II E X P E R I M E N T A L

1. Preparation and Characterization of Hexa-(N,N-dimethylformamido)iron(III) perchlorate.

This water sensitive complex was prepared under vacuum by distillation of N,N-dimethylformamide (DMF) into a flask containing hydrated iron(III) perchlorate (Alpha Inorganics) and molecular sieve (B.D.H., type 3A). The mixture was stirred for 24 hr while under vacuum, then the molecular sieve drying agent was removed by filtration.

The solvent was removed by vacuum distillation until crystallization occurred on cooling in the freezing compartment of a refrigerator overnight. The resulting yellow crystals were collected in a dry nitrogen atmosphere and stored under vacuum. The product was characterized by elemental analysis.

Anal.Calcd for $Fe(DMF)_6(ClO_4)_3$, $FeC_{18}H_{42}Cl_3N_6O_{18}$: C, 27.1%; H, 5.26%; N, 10.5%. Found: C, 27.2%; H, 5.71%; N, 10.7%.

2. Preparation and Characterization of α,β,γ,δ-tetraphenylporphineiron(III) chloride.

The metal free α,β,γ,δ-tetraphenylporphine (TPP) was prepared by the method of Dolphin.[51] Freshly distilled benzaldehyde (Raylo Chemicals Ltd.) and pyrrole were reacted

in refluxing glacial acetic acid. After four hours the acetic acid was removed by vacuum distillation yielding the crude brown product. Purification was achieved by column chromatography on neutral alumina (Fisher Scientific Co.) using chloroform as eluent. The resulting TPP was obtained by slow evaporation of the chloroform solution as a purple powder.

Insertion of iron to produce the desired FeTPPCl complex was achieved by reaction of excess hexaaquoiron(III) chloride (B.D.H., Laboratory Reagent grade) with the purified TPP in refluxing DMF, following the method of Adler et al.[52] Completion of reaction was obtained after about 10 minutes, as evidenced by the absence of visible absorption bands due to the ligand TPP in the electronic spectra of the reaction solution.

The crude product was isolated by adding chilled distilled water and purified by column chromatography on neutral alumina with chloroform as solvent. The chloroform eluate was treated with gaseous hydrogen chloride to ensure that the chloride salt was obtained. Crystallization of this solution was then induced with methanol, producing the purple solid FeTPPCl.

Elemental analysis results for this material were obtained as follows

Anal. Calcd for FeTPPCl.H_2O, $FeC_{44}H_{30}N_4ClO$: C, 73.1%;

H, 4.16%; N, 7.76. Found: C, 72.09%; H, 4.27%; N, 7.24%.

The presence of water in the compound was confirmed by bands at 3200 - 3500 cm^{-1} and 1570 - 1600 cm^{-1} in the infrared spectrum.

The compound was further characterized by visible absorption spectroscopy. The absorption maxima and molar extinction coefficients in benzene solution were observed at 422 nm (9 x 10^4 M^{-1} cm^{-1}), 510 nm (1.3 x 10^4 M^{-1} cm^{-1}) with weaker broad peaks at 590 nm and 700 nm. These results agree with values given in references 53 and 54.

3. Solvent Purification

N,N-dimethylformamide (Raylo Chemicals Ltd.) was first vacuum distilled from barium oxide. This distillate was redistilled twice from molecular sieve, retaining the middle fractions, and stored over the drying agent in vacuum.

Anhydrous methanol (Mallinkrodt Analytical Reagent) was similarly doubly distilled and stored under vacuum over molecular sieve. Cyclopentane (Aldrich Reagent) was stored over the molecular sieve and used without further purification.

4. Sample Preparation

Iron(III)perchlorate - DMF Solutions

These solutions were prepared by transferring about

0.05 g of the $Fe(DMF)_6(ClO_4)_3$ complex to a pre-weighed flask in a nitrogen filled dry-bag, reweighing the evacuated vessel, then vacuum distilling about 2 g of purified DMF into the flask and weighing again.

An aliquot of this solution was poured under vacuum into a 5 mm o.d. nmr sample tube containing cyclopentane (sufficient to be about 5% by volume). The solution was freeze-thaw degassed using liquid nitrogen and finally sealed under vacuum.

Iron(III)porphyrin perchlorate - DMF, Methanol Solutions

Iron(III)porphyrin perchlorate solutions were prepared *in situ* from the chlorides according to the following equation

$$ClFe^{III}Por + AgClO_4 \xrightarrow{S} SFe^{III}Por^{+}ClO_4^{-} + AgCl$$

where Por ≡ TPP or porphine

and S ≡ DMF, methanol.

These solutions were prepared under vacuum to eliminate the presence of water. Typically, about 0.15 g of iron(III)porphyrin chloride was taken together with sufficient $AgClO_4$ to precipitate all the chloride. When a hydrated porphyrin was used, about a gram of molecular sieve was also added and methanolic solutions required the

the addition of a few milligrams of anhydrous 2,4-dinitrobenzene sulfonic acid (Eastman Organic) to collapse any coupling in the methanol spectra.

The solids were pumped for several hours to remove possible traces of water. After this about 0.5 - 2 g of solvent, depending on the amount of line broadening required and the solubility of the porphyrin, was added under vacuum. The cyclopentane nmr reference was generally distilled into the solution before an aliquot was decanted and sealed into an nmr sample tube (5 mm o.d.). When a 100 MHz nmr sample was required, hexamethyldisilane (HMDS) was also added (about 10% by volume) to provide a sharper reference signal for "locking-on" purposes.

5. Instrumentation

The nmr spectra were run on Varian A56/60 and HA-100 spectrometers equipped with V-4343 temperature controllers. The temperatures were determined from the peak separation in methanol or ethylene glycol calibrated standard samples, for 60 MHz spectra. Some temperatures on the HA-100 spectrometer were checked using either a Doric thermocouple thermometer or copper-constantan thermocouple with a potentiometer.

The line widths of the pure solvent were determined immediately after the paramagnetic sample with the same temperature settings, on the Varian 56/60. Special atten-

tion was paid to signal phasing and saturation to ensure truly Lorentzian absorption signals were obtained.

Routine electronic spectra were measured on a Bausch and Lomb Spectronic 505 spectrophotometer, whilst extinction coefficients were obtained using a Cary Model 14 spectrophotometer. Infrared spectra were measured using a Perkin Elmer model 421 spectrophotometer, using KBr discs.

CHAPTER III

NMR Line Broadening and Chemical Shift Studies of Iron(III) and Iron(III)-Porphyrin Systems

1. NMR Line Broadening Study of Hexa(N,N-dimethylformamido) iron(III) perchlorate in N,N-dimethylformamide

This study was undertaken to provide exchange rate data for the hexasolvated metal ion to compare with that of the monosolvated iron(III) porphyrin complexes. The well defined outer-sphere contribution to line broadening in this system aided interpretation of the α,β,γ,δ-tetraphenylporphineiron(III) system, where it will be shown that outer-sphere data was limited. The analysis of the DMF methyl nmr absorption signals will also be presented.

The line broadening data $(T_{2P}P_M)^{-1}$ for $Fe(DMF)_6^{3+}$ in DMF at various temperatures are given in Table 1, and presented in Figure 2. Values have been calculated using a coordination number of six where P_M is given by

$$P_M = 6[Fe]/([DMF] - 6[Fe])$$

$$= 6 \times 73.1 \times 10^{-3} [Fe]$$

and [Fe] is the molal concentration of $Fe(DMF)_6^{3+}$. A recent X-ray structure study [55] performed on $Fe(DMF)_6(ClO_4)_3$ confirmed that Fe(III) is octahedrally coordinated to DMF with each ligand bound through the carbonyl oxygen atom. No

TABLE 1

Proton Line Broadening for $Fe(DMF)_6(ClO_4)_3$ in N,N-Dimethylformamide (60 MHz)

10^2 x complex concn, m	t, °C	$10^3/T$, $°K^{-1}$	$\Delta\nu_{obsd}$, Hz			$(T_{2P}P_M)^{-1} \times 10^{-3}$ sec^{-1}		
			-CH	$-CH_3$ (low field)	$-CH_3$ (high field)	-CH	$-CH_3$ (low field)	$-CH_3$ (high field)
4.01	120	2.545	36.5	25.7	26.8	6.52	4.59	4.78
	100	2.681	18.7	14.2	12.6	3.34	2.54	2.25
	80	2.833	12.9	8.35	9.35	2.30	1.49	1.67
	60	3.003	9.10	6.50	7.84	1.63	1.16	1.40
	46	3.135	9.80	5.01	5.94	1.75	0.895	1.06
	40	3.195	8.40	5.00	6.89	1.50	0.893	1.23
	17.5	3.328		6.33	8.29		1.13	1.48
	-7.0	3.759	19.9	10.8	12.4	3.58	1.93	2.22
	140	2.421	70.4			12.6		
	110	2.611	26.6			4.75		
	28	3.322	9.00			1.61		
2.02	118	2.558		11.3	11.5		4.00	4.06
	105	2.646		6.33	6.84		2.24	2.42
	90	2.755		4.32	4.72		1.53	1.67
	33	3.268	5.40	2.53	3.70	1.93	0.895	1.31
	22	3.390	6.10	3.36	4.72	2.16	1.19	1.67
	-28	4.082		6.33	8.65		2.24	3.06
	-29	4.098		7.40	10.1		2.62	3.56
	-37	4.237	34.3	9.89	11.1	6.12	3.50	3.93
2.11	-16	3.891		4.71	7.18		1.60	2.44
	-27	4.062		6.41	9.44		2.18	3.21
	-48	4.444	21.5	12.6	13.2	7.31	4.30	4.48
	-40	4.292	20.4			6.94		
8.47	37	3.226	21.4			1.81		
	14	3.490	23.0			1.94		

(continued.....)

TABLE 1 (continued)

8.47	13	3.497	29.0			2.45		
	2	3.636	33.0			2.79		
0.347	42	3.175	0.80			1.64		
	50	3.096	0.80	4.48	5.66	1.64	0.800	1.01

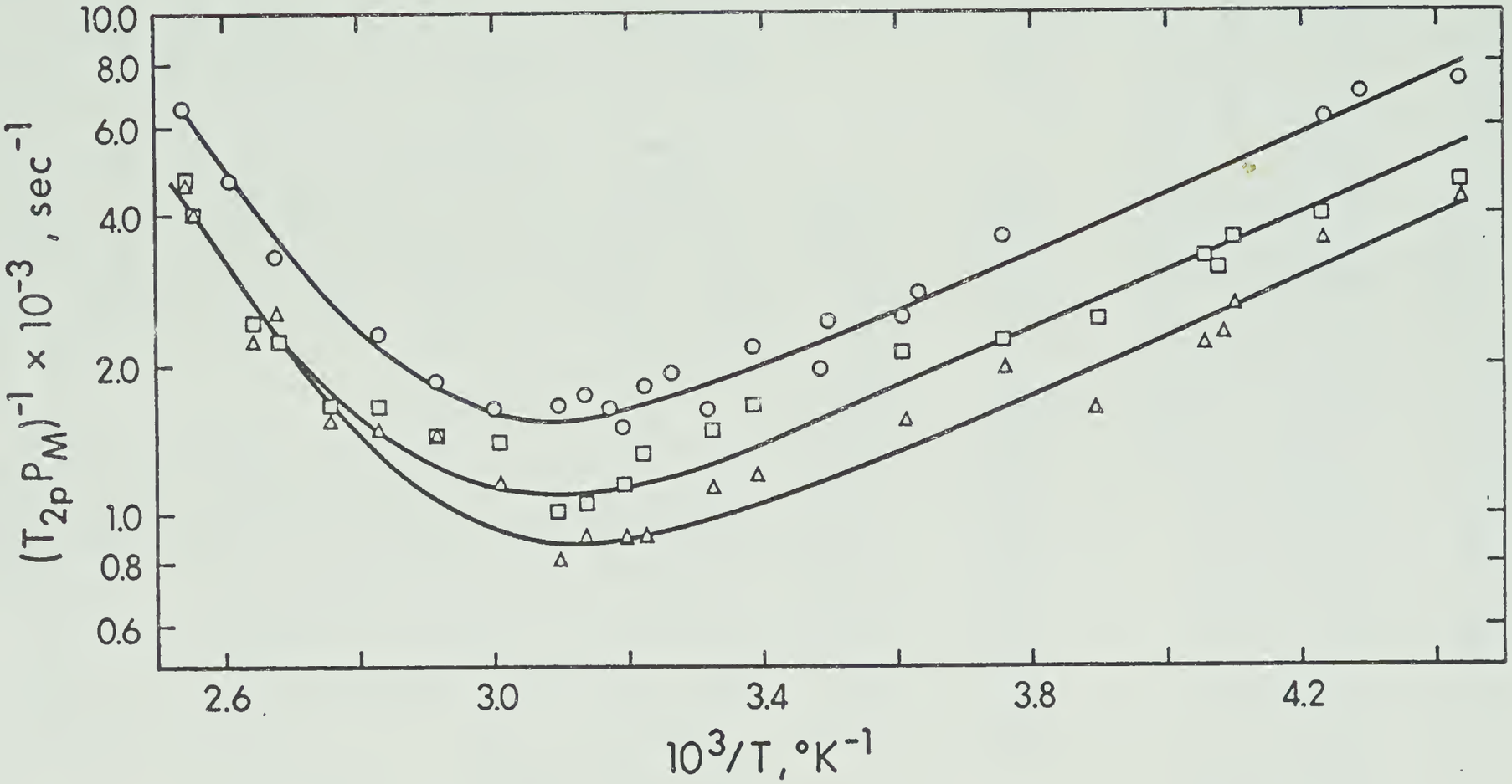

FIGURE 2. Temperature dependence of $-\log(T_{2P}P_M)$ for solutions of $Fe(ClO_4)_3$ in N,N-dimethylformamide. Smooth curves are calculated from fits with $\Delta H^{\ddagger} = 9.98$ kcal mol^{-1} (Table 2) for CH (○), high field CH_3 (□) and lower field CH_3 (△) protons.

solvent shift ($\Delta\omega_{obsd}$) was found for the temperature range studied.

Direct determination of $(T_{2P})^{-1}$ from the methyl proton portion of the spectra is complicated by the overlap of the two broadened lines. The nmr absorption was analysed as a sum of two Lorentzian curves;

$$I_{obs} = \frac{C}{(T_{2P})_1^{-1} + 4\pi^2(T_{2P})_1((\nu_o)_1 - \nu)^2} + \frac{C}{(T_{2P})_2^{-1} + 4\pi^2(T_{2P})_2((\nu_o)_2 - \nu)^2} \quad (37)$$

where I_{obs} is the observed intensity at any frequency, ν; $C = (I_o)_1 \times (T_{2P})_1^{-1} = (I_o)_2 \times (T_{2P})_2^{-1}$; $(T_{2P})_1^{-1}$ and $(T_{2P})_2^{-1}$ are the resolved linewidths at half peak heights; $(I_o)_1$ and $(I_o)_2$ are the peak heights of each resolved methyl resonance; $(\nu_o)_1$ and $(\nu_o)_2$ are the resonance frequencies of each resolved methyl absorption.

About twenty (I_{obs}, ν) coordinates were taken from each observed spectrum and fitted to equation 37, using a non-linear least squares computer program to obtain best-fit values for C, $(T_{2P})_1^{-1}$, $(T_{2P})_2^{-1}$, (ν_o), and $(\nu_o)_2$. The methyl line broadening data shown in Figure 2 and Table 1 is based on $(T_{2P})_1^{-1}$ and $(T_{2P})_2^{-1}$ obtained by this procedure and then treated in an analogous way to the formyl proton data.

Figure 2 indicates that $(T_{2P}P_M)^{-1}$ is controlled by the solvent exchange rate above about 60°C and by outer-sphere relaxation below about 40°C. A simplified form of the Swift and Connick line broadening equation (equation 17) can therefore be applied,

$$(T_{2P}P_M)^{-1} = \tau_M^{-1} + T_{2O}^{-1} \qquad (38)$$

The results of computer fitting the data to this equation are summarised in Table 2 where $\Delta H^{\ddagger}$, $\Delta S^{\ddagger}$ are related to τ_M^{-1} and E_O, C_O are related to T_{2O}^{-1}, as discussed in Chapter 1.

The results for the formyl (CH) proton are considered to be more accurate because the line broadenings are larger and they are not subject to any error which might result from the least-squares resolution of the two methyl (CH_3) linewidths. For this reason, the $\Delta H^{\ddagger}$ and E_O from the CH proton fit were fixed in one of the fits of the CH_3 proton data. The calculated smooth curves in Figure 2 clearly show that the latter fits are consistent with the CH_3 proton data. This is further indicated by the fact that the $\Delta S^{\ddagger}$ values are in good agreement when $\Delta H^{\ddagger}$ is fixed at 9.98 kcal mol^{-1}.

Thus, taking the average of values in Table 2, the exchange between Fe(III) and solvent DMF has $\Delta H^{\ddagger} = 10.1 \pm 1$ kcal mol^{-1}, $\Delta S^{\ddagger} = -16.5 \pm 3$ cal mol^{-1} deg^{-1}, and hence the

TABLE 2

Least-Squares Best-Fit Parameters for

$Fe(DMF)_6(ClO_4)_3$ in DMF

	$\Delta H^{\ddagger}$ kcal mol^{-1}	$\Delta S^{\ddagger}$ cal mol^{-1} deg^{-1}	C_O sec^{-1}	E_O kcal mol^{-1}
CH proton	9.98	-16.4	20.6	2.66
CH_3, low field	9.15	-19.4	12.6	2.57
	9.98[a]	-17.2	10.8	2.66[a]
CH_3, high field	11.4	-13.8	33.5	2.22
	9.98[a]	-17.3	14.3	2.66[a]

[a] Fixed at value indicated by CH proton fit.

reciprocal of the lifetime (τ_M^{-1}) of one solvent molecule in the first coordination sphere is 61 sec^{-1} at 25°C.

The Fe(III)-proton distances [55] for $Fe(DMF)_6^{3+}$ are calculated to be

Fe-CH	3.1 Å
$Fe-CH_3$(cis)	6.4 Å
$Fe-CH_3$(trans)	5.7 Å

if a C-H bond length of 1.08 Å is assumed, and the positions of the iron and carbon atoms are those given from the X-ray crystal structure of $Fe(DMF)_6(ClO_4)_3$. This infers a value of ~6.4 Å for the ionic radius of the complex. If this is also the outer-sphere interaction distance (r_o) for the formyl protons, the value of 1.83×10^3 sec^{-1} for $(T_{2O})^{-1}$ at 25°C calculated with E_o = 2.66 kcal mol^{-1} and C_o = 20.6 sec^{-1}, gives a dipolar interaction correlation time of 1.25×10^{-10} sec at 25°C, using equations 35 and 36. This compares favorably with values found for VO^{2+} in DMF of 1.15×10^{-10} sec [56] and MnB in DMF of 1.27×10^{-10} sec.[57] It is inferred that these correlation times correspond to rotational tumbling of the DMF molecule.

If the cis and trans methyl protons of outer-sphere DMF molecules also have a rotational correlation time of 1.25×10^{-10} sec at 25°C,

where:

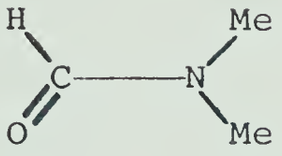

(cis) [Low field nmr resonance]

(trans) [High field nmr resonance]

outer-sphere interaction distances of 7.1 Å for the cis methyl protons and 6.8 Å for the trans methyl protons are consistent with $C_O = 10.8\ sec^{-1}$ and $C_O = 14.3\ sec^{-1}$, respectively. These distances are quite short, placing the cis methyl protons 0.7 Å from the first coordination sphere and the trans methyl protons 0.4 Å. This implies that the second coordination sphere DMF molecules are relatively unstructured and oriented essentially randomly with respect to the $Fe(DMF)_6^{3+}$ ion. It should be noted that this conclusion is independent of the correlation time calculations and results simply from the fact that the outer-sphere broadening is very similar for all three groups of protons in this system.

2. Nmr Line Broadening and Shift Study of α,β,γ,δ-tetraphenylporphineiron(III) perchlorate in N,N-dimethylformamide.

Solutions of α,β,γ,δ-tetraphenylporphineiron(III) perchlorate in DMF were prepared as outlined in Chapter 2. Fe(TPP)Cl is quite soluble in DMF, in the presence of $AgClO_4$, and yields dark brown solutions which give constant

nmr linewidth and shift results over periods of many months.

Tables 3, 4 and 5 contain the observed line broadening and shift results, where it is assumed that only one solvent molecule is coordinated by the high spin $Fe(TPP)^+$ ion. For one exchanging DMF molecule,

$$P_M = [Fe(TPP)^+]/[Solvent]_{pure} - [Fe(TPP)^+]$$

$$= 73.1 \times 10^{-3} \times [Fe(TPP)^+],$$

where $[Fe(TPP)^+]$ is the molal concentration of the complex.

The CH proton 60 MHz results were computer fitted to the two site Swift and Connick equations (equations 17 and 18) containing the temperature dependent functions for each term (equations 19, 21, 32, 36). Since only a limited outer-sphere $(T_{2O})^{-1}$ region could be observed before the samples solidified at low temperatures, accurate C_O and E_O values are difficult to obtain. In the fitting procedures, a value of E_O = 2.66 kcal mol^{-1}, obtained from the $Fe(DMF)_6^{3+}$ system, was used. This E_O also is consistent with values in the range of 2.3 - 2.8 kcal mol^{-1} found for $Ni(TAAB)^{2+}$ in DMF.[58]

Preliminary analysis of the linewidth data was achieved by setting $C_\omega = O$. This procedure was justified since $\Delta\omega_M^2$ only makes a 10 - 15% contribution to the CH proton linewidth data near the maximum of the curve. The preliminary fit of the shift data using $\Delta H^\ddagger$, C_M and E_M values

TABLE 3

Proton Line Broadening for $Fe(TPP)(ClO_4)$ in DMF at 60 MHz and 100 MHz(*)

10^2 x complex concn molal	t, °C	$\frac{10^3}{T}$, $°K^{-1}$	$\Delta\nu_{obsd}$ CH, Hz	$\Delta\nu_{obsd}$ CH_3(cis) Hz	$\Delta\nu_{obsd}$ CH_3(trans) Hz	10^{-4} x $(T_{2P}P_M)^{-1}$, sec^{-1} CH	CH_3 (cis)	CH_3 (trans)
1.238	44.0	3.155	12.3	1.75	3.01	4.63	0.609	1.05
	53.0	3.067	11.2			3.89		
	72.0	2.899	10.5			3.65		
	63.0	2.976	10.1	0.87	3.69	3.51	0.302	1.28
	-22.0	3.984	18.6			6.46		
	-43.0	4.349	9.9			3.44		
	-41.0	4.310	11.4	6.57	5.00	3.96	2.28	1.74
	-46.0	4.405	9.0	6.70	4.94	3.13	2.33	1.72
	-34.0	4.184	15.4			5.35		
*	20	3.413	14.5	7.60	10.4	5.035	0.817	1.12
*	10	3.534	16.9	7.66	10.8	5.868	0.824	1.16
*	-10	3.802	21.6	14.6	12.5	7.500	1.57	1.34
1.080	44.0	3.155	10.3			4.10		
	53.0	3.067	9.7	1.62	3.43	3.86	0.644	1.37
	80.0	2.833	7.9			3.14		
	42.0	3.175	11.0	0.85	3.27	4.30	0.337	1.30
	-10.0	3.802	17.8			6.77		
	26.5	3.339	11.0	1.16	4.16	4.38	0.461	1.66
	22.5	3.384	12.5	1.94	2.83	4.98	0.728	1.13
	18.0	3.436	12.6	1.97	2.96	5.01	0.783	1.18
	14.0	3.484	12.7	2.46	3.11	5.05	0.981	1.24
	9.0	3.546	13.7	2.79	2.81	5.45	1.11	1.12
	4.0	3.610	15.8	4.16	4.05	6.29	1.64	1.61
	0.0	3.663	14.8	3.06	3.88	5.89	1.22	1.54
	-4.0	3.717	16.9	1.93	4.38	6.33	0.767	1.74
	-11.0	3.817	17.5	4.40	4.01	6.97	1.75	1.60
	-17.0	3.906	17.1	2.64	2.92	6.81	1.05	1.16

TABLE 3 (continued)

1.080	-20.0	3.953	17.1	3.57	3.79	6.81	1.42	1.51
	-24.0	4.016	17.2	3.87	3.49	6.85	1.54	1.39
	-25.0	4.032	15.7	6.59	4.34	6.25	2.62	1.73
	43.0	3.165	10.3	2.33	1.40	4.10	0.929	0.557
	37.0	3.226	10.9	1.83	3.56	4.34	0.727	1.42
	-35.0	4.202	12.6	5.75	4.18	5.01	2.29	1.66
	-40.0	4.292	9.9			3.94		
	-46.0	4.405	8.5			3.38		
	-52.0	4.525	6.6			2.63		
	-55.0	4.587	6.1	5.46	3.78	2.43	2.17	1.50
	80.0	2.833	7.9			3.14		
	90.0	2.755	7.3			2.90		
	100	2.681	7.2			2.87		
	110	2.611	7.1			2.82		
	120	2.545	7.0			2.78		
3.996	42.0	3.175	38.3	5.66	8.63	4.12	0.609	0.929
	50.0	3.067	38.2	5.16	8.66	4.11	0.555	0.932
	60.0	2.976	34.1	3.98	7.65	3.67	0.428	0.822
	-55.0	4.587	23.6			2.54		
	-55.0	4.587	24.1			2.60		
	-60.0	4.695	22.6	21.2	8.21	2.43	2.28	0.883
	-46.0	4.405	29.1			3.13		
	-63.0	4.762	23.3			2.50		
	-29.0	4.098	59.2	18.1	13.2	6.37	1.95	1.42
	-39.0	4.274	41.4	26.0	12.8	4.45	2.80	1.37
	-48.0	4.444	29.5	8.89	12.0	3.17	0.956	1.30
	-58.0	4.651	21.7			2.33		
	-11.0	3.817	68.0			7.31		
	-17.0	3.906	63.1			6.79		
	-51.0	4.505	24.6	26.4	11.0	2.65	2.83	1.18
	-50.0	4.484	26.5	27.6	11.5	2.85	2.97	1.24
	-49.0	4.464	27.0	45.9	15.6	2.90	4.93	1.68
	-43.5	4.357	33.5	38.4	18.3	3.60	4.13	1.97
	-42.5	4.338	37.4	26.7	14.9	4.02	2.88	1.60

(continued.....)

TABLE 3 (continued)

3.996	-61.0	4.717	21.2			2.28		
	-62.0	4.739	21.5			2.31		
	-64.0	4.785	21.8			2.34		
*	-20.0	3.953	77.1	14.0	11.2	8.29	1.51	1.20
*	0.0	3.663	63.8	10.3	13.3	6.86	1.11	1.43
*	35.0	3.247	44.4	5.86	9.67	4.78	0.63	1.04

TABLE 4

Formyl Proton Chemical Shifts at 60 MHz for Fe(TPP)(ClO_4) in DMF

10^2 x complex concn, molal	t, °C	$\frac{10^3}{T}$, °K^{-1}	C-H Proton	
			$\Delta\omega_{obsd}$, Hz	$\frac{\Delta\omega_{obsd}}{P_M} \times 10^{-4}$ rad sec^{-1}
1.238	53.0	3.067	8.5	5.90
1.080	53.0	3.067	8.5	6.76
	80.0	2.833	7.0	5.58
	26.5	3.339	8.0	6.36
	22.5	3.384	8.5	6.76
	18.0	3.436	8.2	7.00
	14.0	3.484	9.0	7.16
	9.0	3.546	9.3	7.40
	4.0	3.610	9.0	7.16
	0.0	3.663	8.8	7.00
	-4.0	3.717	9.1	7.24
	-11.0	3.817	9.3	7.40
	-17.0	3.906	7.5	5.98
	-20.0	3.953	7.8	6.20
	-25.0	4.032	5.5	4.38
	43.0	3.165	8.5	6.76
	37.0	3.226	8.2	6.52
	-35.0	4.202	3.8	3.02
	-40.0	4.292	2.8	2.22
	80.0	2.833	7.4	5.88
	90.0	2.755	7.4	5.88
	100	2.681	7.7	6.28
	110	2.611	7.4	5.88
3.966	42.0	3.175	30	6.46
	50.0	3.067	28.3	6.08

(continued..)

TABLE 4 (continued)

3.966	60.0	2.976	27.8	5.98
	-29.0	4.098	14.4	3.10
	-39.0	4.274	3.4	0.73
	-39.0	4.274	5.4	1.16
	-11.0	3.817	28.7	6.18
	-17.0	3.906	22.9	4.92
	-42.5	4.338	0	0.00
	-43.5	4.357	0	0.00
	-49.0	4.464	0	0.00

TABLE 5

Methyl Proton Chemical Shifts at 60 MHz for $Fe(TPP)(ClO_4)$ in DMF

10^2 x complex concn., molal	t, °C	$\frac{10^3}{T}$, $°K^{-1}$	CH_3(cis) $\Delta\omega_{obsd}$ Hz	CH_3(trans) $\Delta\omega_{obsd}$ Hz	CH_3(cis) $\frac{\Delta\omega}{P_M}_{obsd}$ x 10^{-4} rad sec^{-1}	CH_3(trans) $\frac{\Delta\omega}{P_M}_{obsd}$ x 10^{-4} rad sec^{-1}
1.238	44.0	3.155	4.82	2.66	3.35	1.85
	63.0	2.976	4.48	2.49	3.11	1.79
	-41.0	4.310	3.51	1.40	2.44	0.972
	-46.0	4.405	2.86	1.21	1.99	0.840
1.080	53.0	3.067	5.14	3.04	4.09	2.42
	42.0	3.175	4.63	2.39	3.69	1.90
	26.5	3.339	4.02	2.28	3.20	1.81
	22.5	3.384	4.44	2.33	3.53	1.85
	18.0	3.436	4.40	2.26	3.50	1.80
	14.0	3.484	4.74	2.53	3.77	2.01
	9.0	3.546	4.26	1.87	3.39	1.50
	4.0	3.610	4.72	2.40	3.76	1.91
	0.0	3.663	4.61	2.32	3.67	1.85
	-4.0	3.717	2.94	1.78	2.34	1.42
	-11.0	3.817	4.54	2.02	3.61	1.61
	-17.0	3.906	4.17	1.77	3.32	1.41

(continued....)

TABLE 5 (continued)

1.080	-20.0	3.953	4.20	2.08	3.34	1.66
	-24.0	4.016	4.46	1.83	3.55	1.46
	-25.0	4.032	3.37	1.72	2.68	1.37
	43.0	3.165	4.90	2.77	3.90	2.21
	37.0	3.226	4.58	2.54	3.65	2.02
	-35.0	4.202	3.95	1.52	3.14	1.21
	-55.0	4.587	1.60	0.40	1.27	0.31

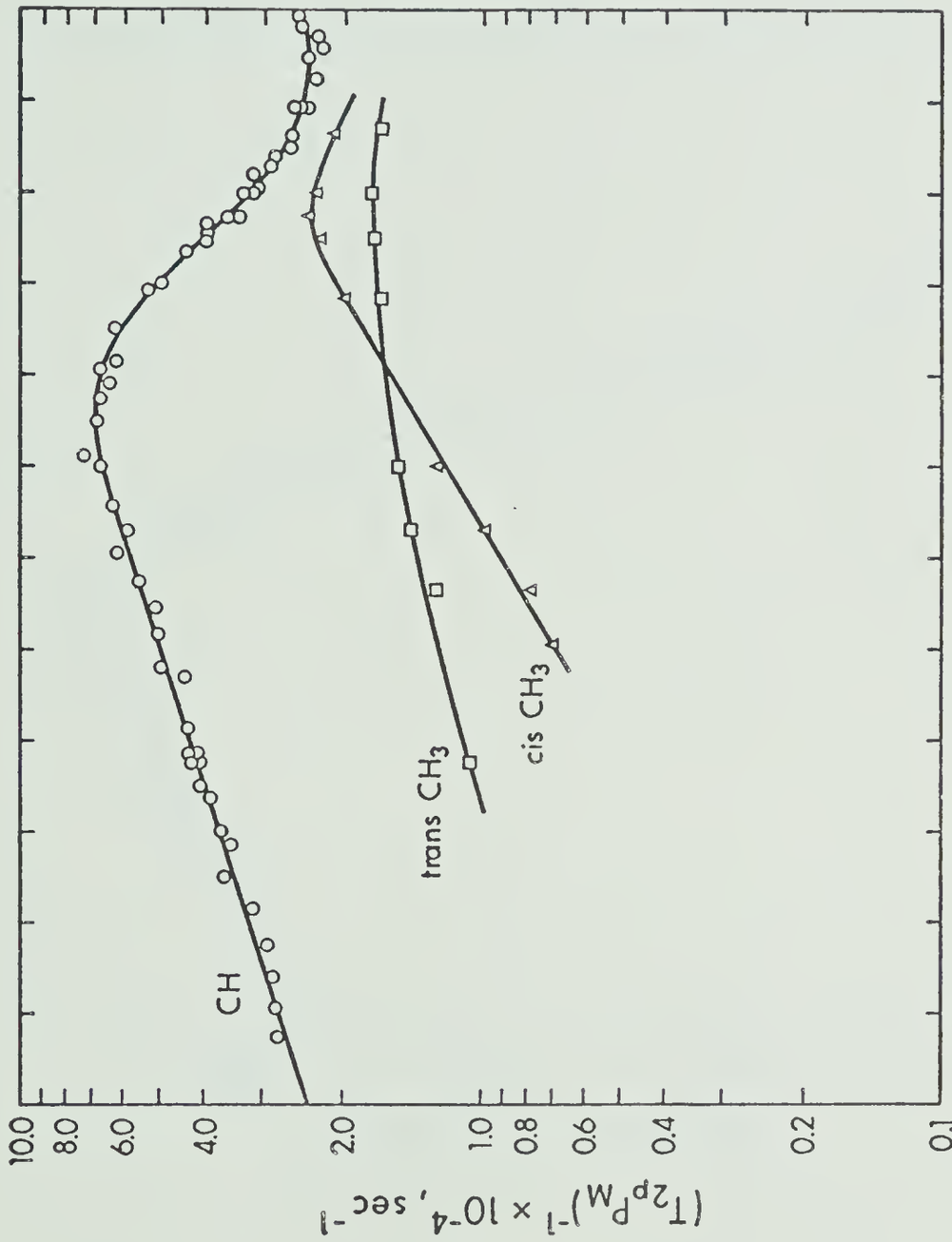

FIGURE 3: Temperature dependence of $-\log(T_{2P}P_M)$ for solutions of $FeTPP^+$ in N,N-dimethylformamide. Smooth curve for CH proton is calculated from fit C (Table 6).

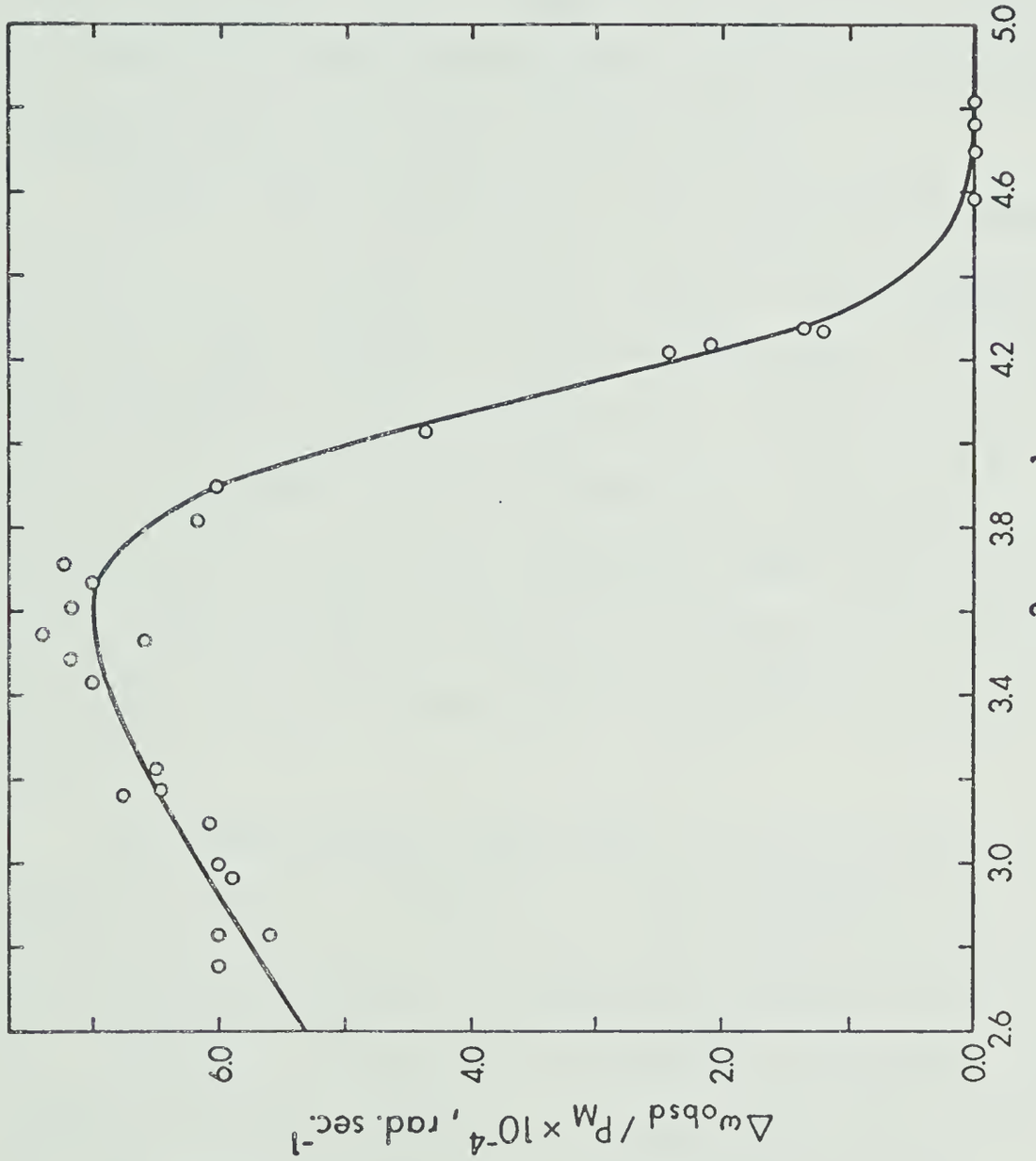

FIGURE 4: Temperature dependence of $\Delta\omega_{obsd}/P_M$ for the CH proton of N,N-dimethylformamide. Smooth curve is calculated from fit E (Table 6).

from the first linewidth fit were used to obtain a C_ω value. Further repetition of this process led to fits C to E shown in Table 6. This method was successful in this case because the shift data is well defined by the limiting chemical shift at high temperatures and hence C_ω is relatively insensitive to the $\Delta H^\ddagger$ and $\Delta S^\ddagger$ values.

Fits A and B illustrate two alternative types of fit. In fit A, the poorly defined $(T_{2O})^{-1}$ data parameters, E_O and C_O, were allowed to vary and are seen to yield an E_O value which is unacceptably high. In fit B, E_M is set equal to E_O and gives a somewhat low value for E_O but is otherwise in reasonable agreement with fits C to E. Fits B to E give average activation enthalpy and entropy values of $\Delta H^\ddagger = 9.4 \pm 0.4$ kcal mol^{-1} and $\Delta S^\ddagger = 3.8 \pm 0.7$ cal mol^{-1} deg^{-1}.

The temperature dependence of $\Delta\omega_{obsd}$ for the formyl proton is shown in Figure 4. The chemical shifts are not sufficiently precise to permit a complete fit to equation 18. However, if C_M and E_M are fixed, then the least-squares fit (D in Table 6) yields values for $\Delta H^\ddagger$ and $\Delta S^\ddagger$ in reasonable agreement with those from the $(T_{2P}P_M)^{-1}$ data. Fit E and the curve drawn in Figure 4 show that the shift and line broadening results are compatible with the same exchange rate parameters. The value of $C_\omega = 2.04 \times 10^7$ radians sec^{-1} deg from Fit E can be used with equation 20 to calculate a value for the hyperfine coupling constant

TABLE 6

Least-Squares Best-Fit Parameters for $Fe(TPP)(ClO_4)$ in DMF, (Formyl Proton Data)

	$(T_{2P}P_M)^{-1}$ data			Δω Data	
	A	B	C	D	E
$\Delta H^{\ddagger}$, kcal mol^{-1}	8.01	9.78	9.37	9.19	9.37[d]
$\Delta S^{\ddagger}$, cal mol^{-1} deg^{-1}	-2.09	4.43	3.11	3.47	4.22
10^{-3} C_M, sec^{-1}	4.16	3.82	4.74	4.74[d]	4.74[d]
E_M, kcal mol^{-1}	1.44	1.37[b]	1.31	1.31[d]	1.31[d]
C_O, sec^{-1}	2.20×10^{-3}	822	36.4		
E_O, kcal mol^{-1}	6.67	1.37[b]	2.66[c]		
10^{-7} C_ω rad sec^{-1} deg	2.04[a]	2.04[a]	2.04[a]	2.05	2.04

[a] Fixed at value indicated by Δω data

[b] E_M set equal to E_O

[c] Fixed at value obtained from $Fe(DMF)_6^{3+}$ system, Table 1.

[d] Fixed at value given by fit C.

$(A/\hbar)$ of $+3.70 \times 10^6$ radians sec^{-1}, based on an effective magnetic moment of 5.9 BM.[33]

Figure 3 is calculated from fit C, which shows the consistency of the parameters from this fit with the observed data. Fit C is also consistent with the formyl proton linewidth data obtained at 100 MHz, as shown in Table 7.

The predicted values are computed using equation 17 and parameters of fit C in Table 6. Insufficient 100 MHz data was obtained to warrant an independent fit of these results.

The inner-sphere relaxation rate $(T_{2M})^{-1}$ of the CH proton is calculated to be 4.32×10^4 sec^{-1} at 25° from the E_M and C_M parameters of fit C and equation 32. This value is consistent with relaxation by the dipolar mechanism [47], for which the first term in equation 22 gives

$$(T_{2M})_{DD}^{-1} = \frac{(\gamma_I g\beta)^2 S(S+1)}{15 r_i^6} \left(7\tau + \frac{13\tau}{1+\omega_s^2\tau^2}\right) \quad . \quad (39)$$

It is found that an inner-sphere interaction distance r_i of 3 Å (indicated by the X-ray studies discussed in section 1 of this Chapter) and a correlation time (τ) of 3.2×10^{-11} sec successfully reproduce the observed values of (T_{2M}^{-1}) at 25°. This correlation time is much shorter than the rotational correlation time of $\sim 1.2 \times 10^{-10}$ sec estimated for vanadyl in DMF.[56] Therefore the correlation time is probably the

TABLE 7

Calculated and Observed 100 MHz Line Broadening Data for the Formyl Proton of N,N-dimethylformamide Solutions of $FeTPP^+$.

t, °C	$10^3/T$, $°K^{-1}$	$(T_{2P}P_M)^{-1} \times 10^4$, sec^{-1}.	
		Calc. (Fit C)	Obsd
20	3.413	5.21	5.04
10	3.535	5.96	5.87
-10	3.802	8.20	7.50
-20	3.953	8.71	8.29
0	3.663	6.97	6.86
35	3.247	4.46	4.78

electron spin relaxation time (τ_e) of the high-spin iron(III) complex. This proposal is consistent with the failure of Wolberg and Manassen [35] to observe a room temperature epr spectrum for $FeTPP^+$. The somewhat low value of E_M is also consistent with this assumption.

The hyperfine (Fermi contact) interaction contribution to $(T_{2M})^{-1}$ has been neglected in the above calculation. This is justified since the hyperfine contribution,

$$(T_{2M})_{HF}^{-1} = \frac{1}{3}(A/\hbar)^2 S(S+1)\left[\tau_{e1} + \frac{\tau_{e2}}{1+\omega_s^2\tau_e^2}\right], \quad (40)$$

is 1.30×10^3 sec^{-1} (at 25°C) for $A/\hbar = 3.7 \times 10^6$ rad sec^{-1} and $\tau \approx 3.2 \times 10^{-11}$ sec. This represents only a 3% contribution to the experimental $(T_{2M})^{-1}$ value, at 25°. Any additional relaxation by a hyperfine interaction mechanism would reduce $(T_{2M})_{DD}^{-1}$ and a smaller value for τ would be computed from equation 39. A smaller τ would result in a smaller $(T_{2M})_{HF}^{-1}$ value. Hence the $(T_{2M})_{HF}^{-1}$ contribution calculated above is an upper limit.

The line broadening results for the methyl protons of DMF are also given in Table 3, and plotted as the lower two curves in Figure 3. These data were obtained by the same method that was used for the $Fe(DMF)_6^{3+}$ system.

These results are not helpful in determining $\Delta H^{\ddagger}$ and $\Delta S^{\ddagger}$, as they show little effect due to chemical exchange. Only the <u>cis</u> CH_3 protons demonstrate a region from about

$10^3/T = 4.2$, $°K^{-1}$ to $10^3/T = 4.5$, $°K^{-1}$, where the exchange rate (τ_M^{-1}) has some effect on the observed line broadening, $(T_{2P}P_M)^{-1}$.

A computer analysis would not be meaningful because of the low accuracy of the linewidth and shift data of the methyl protons, together with the absence of outer-sphere linewidth data. The latter results because the solvent peaks broaden so much that they coalesce at low temperatures. However, it is possible to account qualitatively for the linewidth behaviour using equations 17, 19, 21, 32 and 36.

Table 8 shows $(T_{2P}P_M)^{-1}$ values calculated from estimates of C_M, E_M, C_O and C_ω. It has been assumed that $\Delta H^\ddagger$, $\Delta S^\ddagger$ and E_O are the same for the methyl protons as for the formyl proton (fit C in Table 6).

The values for C_O have been estimated by assuming that the ratio C_O methyl protons : C_O formyl for this system is the same as that found in the $Fe(DMF)_6^{3+}$-DMF system. This ratio is 0.524 for the cis methyl protons and 0.694 for the trans methyl protons.

These calculations successfully show that the major difference in the behaviour of the cis methyl proton $(T_{2P}P_M)^{-1}$ data compared to that of the trans methyl protons can be accounted for by the larger C_ω value for the former. This results in a much greater $\Delta\omega_M^2$ contribution to $(T_{2P}P_M)^{-1}$ for the cis methyl protons and causes the data

TABLE 8

Calculated and Observed Line Broadening Data for the Methyl Protons of DMF Solutions of $FeTPP^+$

Trans-Methyl Protons

t, °C	$10^3/T$, $°K^{-1}$	$(T_{2p}P_M)^{-1} \times 10^{-4}$, sec^{-1}. Calc.[a]	Obsd.
-50.8	4.5	1.8	1.7
-45.7	4.4	1.8	1.75
-40.4	4.3	1.8	1.7
-34.9	4.2	1.7	1.7
4.8	3.6	1.1	1.4

[a] Using: $C_M = 3.3 \times 10^3$ sec^{-1}, $E_M = 0.5$ kcal mol^{-1}, $C_O = 25.3$ sec^{-1}, $C_\omega = 3 \times 10^6$ rad sec^{-1}, ($\Delta H^\ddagger = 9.37$ kcal mol^{-1}, $\Delta S^\ddagger = 3.11$ cal deg^{-1} mol^{-1} and $E_O = 2.66$ kcal mol^{-1}).

Cis-Methyl Protons

t, °C	$10^3/T$, $°K^{-1}$	$(T_{2p}P_M)^{-1} \times 10^{4}$, sec^{-1} Calc.[b]	Obsd.
-50.8	4.5	1.9	2.15
-45.7	4.4	2.2	2.3
-40.4	4.3	2.3	2.3
-34.9	4.2	2.1	2.1
4.8	3.6	0.55	0.53

[b] Using: $C_M = 1 \times 10^3$ sec^{-1}, $E_M = 0.5$ kcal mol^{-1}, $C_O = 19.1$ sec^{-1}, $C_\omega = 8 \times 10^6$ rad sec^{-1} deg, ($\Delta H^\ddagger = 9.37$ kcal mol^{-1}, $\Delta S^\ddagger = 3.11$ cal deg^{-1} mol^{-1} and $E_O = 2.66$ kcal mol^{-1}).

for the latter to increase more rapidly with decrease in temperature than the trans methyl proton data. In this particular system, this increase is sufficient to cause a cross-over of the two curves.

The methyl proton shift data is of low accuracy due to the small shifts observed and the necessity to obtain them from computer fitted curves. Estimated C_ω values from the shift data are 1.1×10^7 rad sec^{-1} and 6.3×10^6 rad sec^{-1} for the cis and trans methyl protons respectively. These values are larger than those used to calculate $(T_{2P}P_M)^{-1}$ in Table 8 and would not give a reasonable fit to the $(T_{2P}P_M)^{-1}$ data. This disagreement is not considered serious in view of the uncertainty in the experimental shift data. The shift data does indicate that C_ω is greater for the cis than for the trans methyl protons, as required to explain the $(T_{2P}P_M)^{-1}$ data.

3. NMR Line Broadening and Shift Study of α,β,γ,δ-tetraphenylporphineiron(III) perchlorate in Methanol

The perchlorate salt of $FeTPP^+$ has a lower solubility in methanol than in DMF. Four samples, prepared as outlined in Chapter 2 Section 4, were studied, with $FeTPP^+$ concentrations in the range 9.2×10^{-3} - 1.5×10^{-2} m. Since line broadenings in the range 5 - 20 Hz and chemical shifts of only 6 Hz were observed, the accuracy of the parameters obtained for system is limited by the

low solubility.

The temperature dependencies of $(T_{2P}P_M)^{-1}$ and $\Delta\omega_{obsd}/P_M$ are given in Tables 9 and 10, and are shown in Figures 5 and 6. Initially the $(T_{2P}P_M)^{-1}$ results fitted to a modified form of equation 17 in which the $\Delta\omega_M^2$ terms were omitted. This gave preliminary values of $\Delta H^{\ddagger}$, $\Delta S^{\ddagger}$, C_M and E_M which were then used with equation 18 to fit the chemical shift $(\Delta\omega_{obsd}/P_M)$ results to determine values for C_ω. This was the same procedure that was used to fit the $FeTPP^+$/DMF results.

Good estimates of C_ω were obtained in this way, since C_ω was not very sensitive to $\Delta H^{\ddagger}$, $\Delta S^{\ddagger}$, C_M and E_M values. The procedure is also justified since the $\Delta\omega_M^2$ terms make <5% contribution to the OH proton $(T_{2P}P_M)^{-1}$ values, although they can affect the CH_3 proton values by about 20%.

The values of C_ω obtained from the $\Delta\omega_{obsd}/P_M$ data were fixed in the $(T_{2P}P_M)^{-1}$ analysis and the complete equation 17 was used to obtain least-squares best-fit values of the other parameters. It should be noted that $\Delta H^{\ddagger}$ and $\Delta S^{\ddagger}$ are best defined by the OH proton $(T_{2P}P_M)^{-1}$ data, in the temperature region $10^3/T = 3.8\ °K^{-1}$ to $10^3/T = 4.2\ °K^{-1}$, that is from -10° to -35° in Figure 5. However, the CH_3 proton results best define E_M in the region $10^3/T = 3.2\ °K^{-1}$ to $10^3/T = 3.9\ °K^{-1}$, that is from 40° to -17°. This can be seen in Table 11 from fits E, F and

TABLE 9

Proton Line Broadening for $Fe(TPP)(ClO_4)$ in Methanol at 60 MHz

10^2 x complex concn molal	t, °C	$\frac{10^3}{T}$, $°K^{-1}$	$\Delta\nu_{obsd}$ OH, Hz	$\Delta\nu_{obsd}$ CH_3, Hz	$10^{-5} \times (T_{2P}P_M)^{-1}$ OH sec^{-1}	$10^{-5} \times (T_{2P}P_M)^{-1}$ CH_3 sec^{-1}
1.052	-77.0	5.102	(2.85)	3.5		0.326
	-61.0	4.717	(2.40)	(2.0)		
	-40.0	4.292	(3.20)	(3.5)		
	40.0	3.195	(15.2)	(3.6)		
	35.0	3.247	16.2	(3.6)	1.51	
	30.0	3.300	16.1_5	3.1	1.51	0.290
	25.0	3.356	16.6_5	(3.6)	1.55	
	20.0	3.413	16.6_5	3.6	1.55	0.336
	15.0	3.472	16.6	3.8	1.55	0.354
	10.0	3.534	16.1	4.0	1.50	0.374
	-10.0	3.802	12.0_5	(6.4)	1.12	
	-18.0	3.922	9.55	6.5	0.892	0.607
	-24.0	4.016	6.70	5.8	0.626	0.548
	-32.0	4.149	4.25	4.5	0.396	0.420
	-44.0	4.367	2.50	(3.0)	0.234	
	-22.0	3.984	7.50	5.8	0.642	0.542
	-31.0	4.132	4.50	(3.7)	0.420	
	-27.0	4.065	5.8	(5.0)	0.542	
	-33.0	4.167	4.0	(3.5)	0.374	
	-43.0	4.348	2.5	2.0	0.234	0.187
0.9526	- 7.0	3.759	12.5_5	4.5	1.29	0.464
	-17.0	3.906	9.0_5	5.5	0.932	0.587
	-27.0	4.065	(6.0)	5.0		0.516
	-38.0	4.255	(4.0)	(3.5)		
	- 3.0	3.745	(12.4)	(4.7)		
	-12.0	3.831	9.8_5	5.5	1.02	0.567
	-18.0	3.922	8.3_5	5.7	0.860	0.588
	-24.0	4.016	6.3_5	(5.3)	0.654	

(continued.....)

TABLE 9 (continued)

0.9526	-32.0	4.149	(4.5)	4.3		0.443
	-44.0	4.367	(3.3)	(3.2)		
	-44.0	4.367	(3.1)	(2.8)		
	-58.0	4.651	(3.4)	(2.9_5)		
	-56.0	4.608	(3.2_5)	(2.7_5)		
	-55.0	4.587	(3.1_5)	(2.5_5)		
	-52.0	4.525	(2.8_5)	(2.6_5)		
	40.0	3.195	(13.0)			
	30.0	3.300	14.0	(2.8)	1.44	
	22.0	3.390	14.0	(3.2)	1.44	
	-49.0	4.464	(3.0)	1.8		0.186
	-63.0	4.762	3.3	2.1	0.340	0.216
	-65.0	4.808	(3.5)	(2.0)		
	-67.0	4.854	(4.0)	2.8		0.289
	-57.0	4.630		(3.0)		
	50.0	3.049	12.0	(1.8)	1.24	
	60.0	2.959	(12.0)	(1.5)		
0.9175	3.0	3.623	13.1	3.8	1.40	0.406
	-11.0	3.817	11.7_5	5.0	1.26	0.536
	-22.0	3.984	8.0_5	5.3	0.662	0.568
	-30.0	4.115	4.8	(5.1)	0.514	
	-42.0	4.329	(3.0)	(2.9)		
	-52.0	4.525	2.3_5	(2.7)	0.252	
	-60.0	4.695	(2.2)	(2.5)		
	-72.0	4.975	(2.5)	2.9		0.310
	-49.0	4.673	2.7	(2.5)	0.290	
	-59.0	4.926	2.8	2.5	0.300	0.268
	-64.0	5.181	3.5	3.0	0.374	0.321
1.532	40.0	3.195	22.0	4.1	1.41	0.262
	0.0	3.663	21.0	6.5	1.35	0.416
	-10.0	3.802	17.0	7.8	1.09	0.500

(continued.....)

TABLE 9 (continued)

1.532	-20.0	3.953	10.8	8.0	0.692	0.512
	-30.0	4.132	5.7	5.1	0.366	0.326
	-40.0	4.292	3.5	3.5	0.224	0.224
	-50.0	4.484	(2.9)	2.7		0.173
	-60.0	4.695	(3.0)	3.0		0.192
	-50.0	4.484	3.5	3.3	0.224	0.212
	-38.0	4.202	5.0	4.6	0.320	0.295
	-25.0	4.032	9.0	7.5	0.577	0.481
	-15.0	3.876	15.0	8.5	0.961	0.545
	- 3.0	3.704	20.5	6.8	1.31	0.436
	18.0	3.436	23.0	5.0	1.47	0.320
	28.0	3.322	(20.0)	4.3		0.276
	40.0	3.195	(21.5)	4.5		0.288

The bracketed values above were rejected from final data fitting because of their large deviations from the best-fit curves.

TABLE 10

Hydroxy and Methyl Proton Chemical Shifts at 60 MHz for $Fe(TPP)(ClO_4)$ in Methanol

10^2 x complex concn, molal	t, °C	$\frac{10^3}{T}$, $°K^{-1}$	$\Delta\omega_{obsd}$ -OH, Hz	$\Delta\omega_{obsd}$ $-CH_3$, Hz	$\frac{\Delta\omega_{obsd}}{P_M} \times 10^{-4}$ -OH, $rad\ sec^{-1}$	$-CH_3$ $rad\ sec^{-1}$
1.052	40	3.195		4.0		6.41
	35	3.247		4.5		7.21
	25	3.356		4.0		6.41
	15	3.472		4.5		7.21
	10	3.534		4.0		6.41
	-10	3.802		3.5		4.00
	-18	3.922		2.5		2.40
	-24	4.016		1.5		1.60
0.9526	- 7	3.759		3.0		6.18
	-17	3.906		2.5		5.15
	-27	4.065		1.0		2.06
	- 3	3.704		2.7		5.57
	-12	3.831		2.2		4.54
	-18	4.016		0.7		1.44
	40	3.195		3.5		7.22
	30	3.300		3.2		6.60
	60	2.959		3.4		7.00
	-38	4.255		0.50		1.03
0.9175	3	3.623		3.0		6.42
	-11	3.817		2.5		5.25
	-22	3.984		2.0		4.28
	-30	4.115		0.5		1.07

(continued.....)

TABLE 10 (continued)

1.532	40	3.195		5.4		6.92
	0	3.663	2.9	4.8	3.72	6.16
	-10	3.802	3.4	4.0	4.36	5.12
	-20	3.953	1.3	1.0	1.67	1.28
	-15	3.876		2.6		4.10
	- 3.0	3.704		4.3		6.28
	18	3.436	5.7	5.2	7.31	7.44
	28	3.322		5.0		7.18
	40	3.195	6.7	5.5	8.59, 7.30	7.82
	60	3.003	4.5		5.77	
	55	3.049	5.2		6.67	
	49	3.106	5.0		6.41	
	45	3.145	6.3		8.08	
	-60	4.695	1.0		1.28	
	-50	4.484	0.4		0.512	
	57	3.030			7.70	

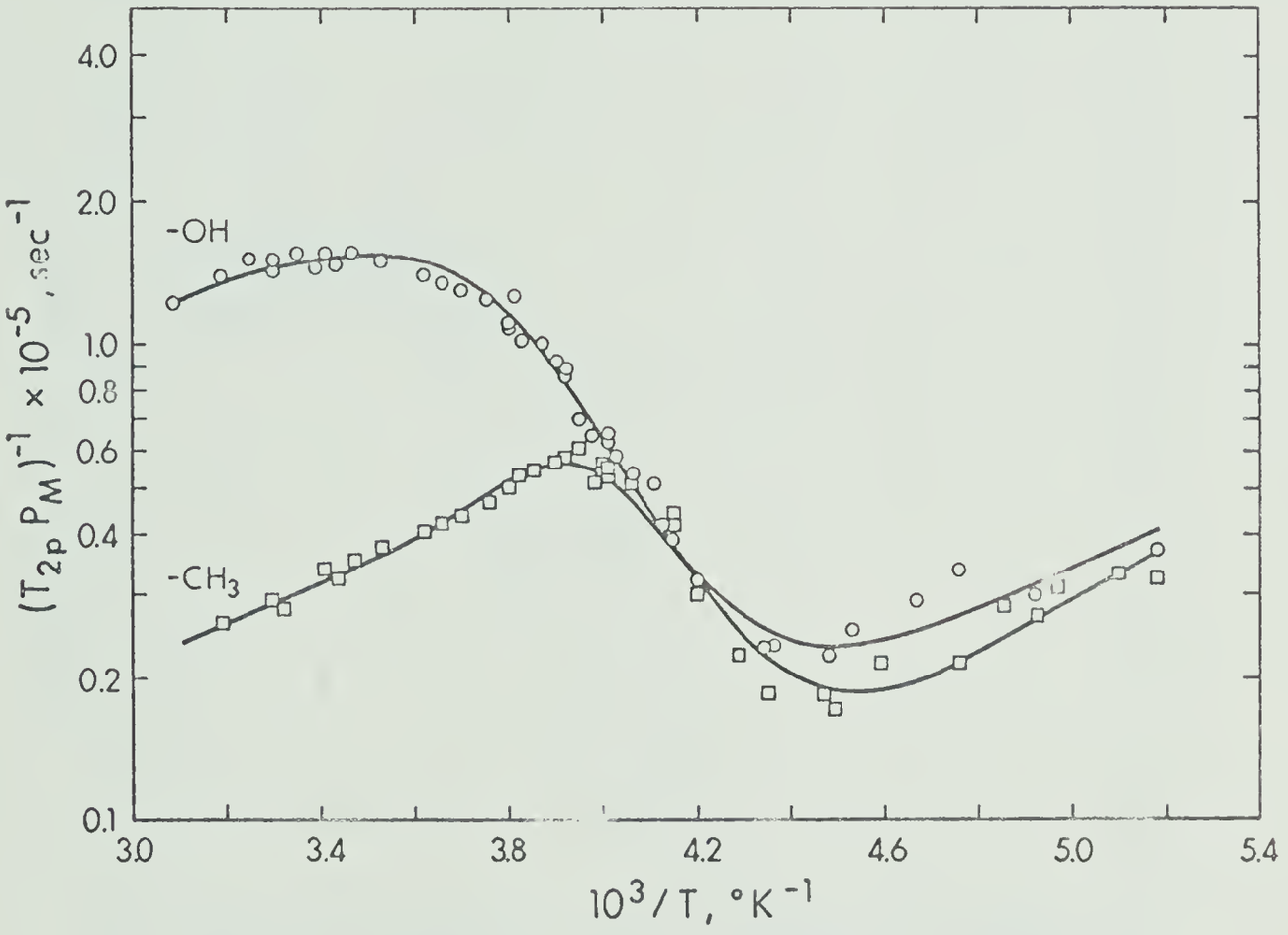

FIGURE 5: Temperature dependence of $-\log(T_{2P}P_M)$ for solutions of $FeTPP^+$ in methanol. Smooth curves are calculated from fits D and G (Table 11).

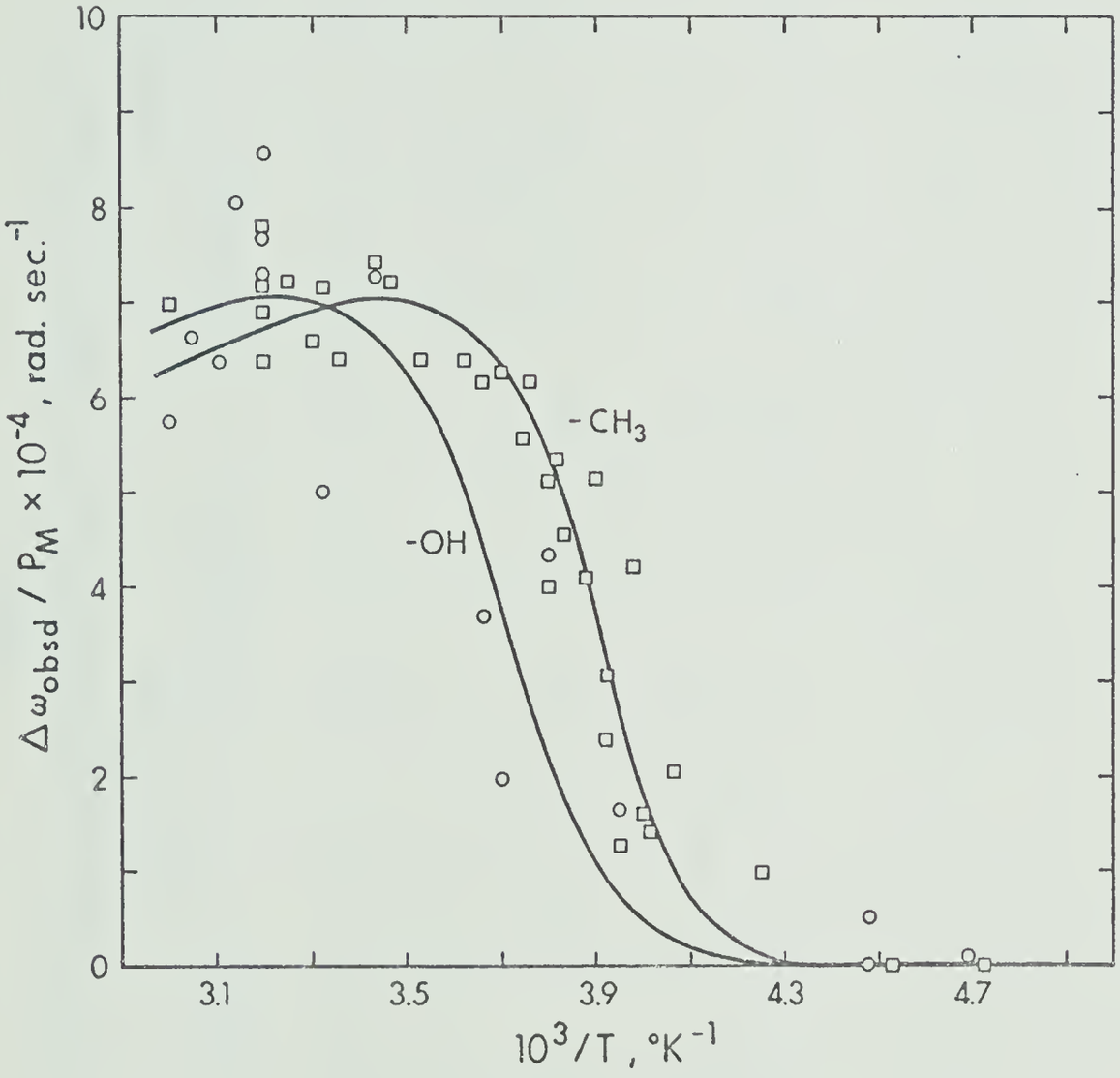

FIGURE 6: Temperature dependence of $\Delta\omega_{obsd}/P_M$ for solutions of $FeTPP^+$ in methanol. Smooth curves are calculated from fits I and L (Table 11).

TABLE 11

Least-squares Best-fit Parameters for $FeTPP^+$ in Methanol

	$(T_{2P}P_M)^{-1}$ Data							Δω Data				
	OH Proton				CH_3 Protons			OH Proton		CH_3 Protons		
	A	B	C	D	E	F	G	H	I	J	K	L
$\Delta H^{\ddagger}$, kcal mol^{-1}	11.63	12.89	11.37	11.28	12.89[f]	11.63[h]	11.28[j]	11.62[a]	11.28[j]	11.63[h]	12.89[f]	11.28[j]
$\Delta S^{\ddagger}$, cal $mol^{-1}deg^{-1}$	10.17	15.51	9.32	8.97	16.09	10.95	9.52	10.28	8.98	10.36	15.2	8.92
$10^{-2} \times C_M$, sec^{-1}	97.5	575	162	150	28.4	26.3	25.7	97.4[a]	150[j]	6.03[g]	28.4[d]	25.7[k]
E_M, kcal mol^{-1}	1.59[c]	0.53	1.30[d]	1.35[e]	1.30	1.35	1.37	1.59[a]	1.35[j]	2.14[g]	1.30[d]	1.37[k]
C_0, sec^{-1}	577	315	192	186	65.5	40.2	34.2	-	-	-	-	-
E_0, kcal mol^{-1}	1.59[c]	1.86	2.05	2.06	2.42	2.61	2.68	-	-	-	-	-
$10^{-7} \times C_\omega$, sec^{-1}	2.27[b]	2.27[b]	2.27[b]	2.27[b]	2.11[g]	2.10[i]	2.10[i]	2.27	2.28	2.10	2.08	2.12

(a) Fixed at value from preliminary fit neglecting $\Delta\omega_M^2$ terms. (b) Fixed at value from fit H. (c) E_M set equal to E_0. (d) Fixed at value from fit E. (e) Fixed at value from fit F. (f) Fixed at value from fit B. (g) Fixed at value from preliminary fit not shown. (h) Fixed at value from fit A. (i) Fixed at value from fit J. (j) Fixed at value from fit D. (k) Fixed at value from fit G.

G which show that E_M for the CH_3 protons is relatively insensitive to the $\Delta H^{\ddagger}$ and $\Delta S^{\ddagger}$ values.

It has been assumed that E_M is the same for both the OH and CH_3 protons, and therefore that the E_M from fit B is meaningless because the value is poorly defined by the OH proton line broadening data at high temperatures. The fitting was continued until reasonable self-consistency of E_M and $\Delta S^{\ddagger}$ was obtained as represented by fits D and G, and then final fits I and L of the shift data were obtained.

Smooth curves for the $(T_{2P}P_M)^{-1}$ and $\Delta\omega_{obsd}/P_M$ shown in Figures 5 and 6 have been drawn based on the parameters given in the final fits D, G, I and L. Whilst the main assumption which has been used in evaluating the results is that E_M is the same for both the OH and CH_3 protons, the results for the two CH_3 protons in the $FeTPP^+$ - DMF system casts some doubt on this assumption. Thus, it is not possible to completely disregard fit B which gave $\Delta H^{\ddagger}$ = 12.9 kcal mol^{-1} and $\Delta S^{\ddagger}$ = 15.5 cal mol^{-1} deg^{-1}. However, using equation 19 the latter parameters give τ_M^{-1} (25°) = 5.3 x 10^6 sec^{-1}, not qualitatively different from the value of 3.1 x 10^6 sec^{-1} calculated from $\Delta H^{\ddagger}$ = 11.28 kcal mol^{-1} and $\Delta S^{\ddagger}$ = 9.0 cal mol^{-1} deg^{-1} (from fits D, I and L).

The chemical shift results, which are shown in Figure 6, are not very accurate because the maximum observable shift was only 6 Hz. The shifts show the ex-

pected temperature dependence and have been fitted to equation 18 in fits H to L as described above. The C_ω values in Table 11 can be used to calculate hyperfine coupling constants ($A/\hbar$) of $+1.4 \times 10^6$ sec^{-1} and $+1.3 \times 10^6$ sec^{-1} for the hydroxy and methyl protons, respectively, using equation 20 and a value of $\mu_{eff} = 5.9$ BM.[33]

The results from fits D and G predict inner-sphere relaxation rates, $(T_{2M})^{-1}$, of 1.47×10^5 and 2.58×10^4 sec^{-1}, using equation 32, for the hydroxy and methyl protons, respectively. Equation 39 shows that these results are consistent with relaxation by a dipolar mechanism with interaction distances (r_i) of 3.0 and 4.0 Å for the hydroxy and methyl protons, respectively, and a correlation time (τ) of 1.06×10^{-10} sec. The calculated T_{2M}^{-1} values are then 1.46×10^5 sec^{-1} for the OH proton and 2.61×10^4 sec^{-1} for the CH_3 protons. The correlation time is three times longer than that found in DMF and could be either the electron spin relaxation time or the rotational tumbling time of the molecule.

4. NMR Line Broadening Study of Porphineiron(III) perchlorate in Methanol

Porphineiron(III) chloride, as obtained from the Mad River Chemical Co., was used without further purification. Three sample solutions were prepared, as outlined in Chapter II, of the sparingly soluble porphineiron(III)

perchlorate ($FePor^+ClO_4^-$) in methanol. The low solubility of the porphine complex somewhat limits the accuracy of this study, particularly the shift data where the maximum observed shift was 12 Hz. The methyl linewidth data is also of low accuracy since the maximum observed linewidth was only 8 Hz.

The proton line broadening results are presented in Table 12 and Figure 7, and the chemical shift data in Table 13 and Figure 8. Comparison with the $FeTPP^+$-methanol system discussed in the previous section (Figures 5 and 6), shows these two systems have similar $(T_{2P}P_M)^{-1}$ and $\Delta\omega_{obsd}/P_M$ versus temperature curves. Thus an analysis of the data of the $FePor^+$-methanol system was attempted in a manner similar to that of the $FeTPP^+$-methanol system.

Table 14 shows the results of the various fits applied to the data. It was decided to constrain the value of $E_M = E_O$ for the final fits. The value chosen for E_M and E_O was 1.88 kcal mol^{-1} as indicated by fit A. This value is consistent with that found in the $FeTPP^+$ study, where an E_O in the range 1.59 - 2.68 kcal mol^{-1} was indicated. An $E_O = E_M$ value of 2.0 kcal mol^{-1} has also been found in the $Mn(DMPrPor)ClO_4$-methanol system.[1]

The methyl linewidth data is very sensitive to the choice of C_ω. A qualitative analysis of this data indicates that a smaller C_ω than that obtained from the shift data would give a better fit to the observed data than has

TABLE 12

Proton Line Broadening for $FePorClO_4$ in Methanol (60 MHz)

10^2 x complex concn molal	t, °C	$10^3/T$ $°K^{-1}$	$\Delta\nu_{obsd}$, Hz -OH	$\Delta\nu_{obsd}$, Hz $-CH_3$	$(T_{2p}P_M)^{-1} \times 10^{-4}$, sec^{-1} -OH	$(T_{2p}P_M)^{-1} \times 10^{-4}$, sec^{-1} $-CH_3$
3.449	30	3.300	15.4	2.9	4.38	0.825
	20	3.413		4.3		1.22
	10	3.534	16.3	6.2	4.64	1.76
	0	3.663	13.3	6.2	3.79	1.76
	40	3.195	14.5	3.0	4.13	0.854
	50	3.096	12.0	2.0	3.42	0.569
	60	3.003	10.6	1.6	3.02	0.455
	64	2.967	9.9	1.6	2.82	0.455
	55	3.049	11.1	2.1	3.16	0.598
	45	3.145	12.8	2.5	3.64	0.712
3.672	- 2	3.690	13.3	5.7	3.56	1.52
	-12	3.831	9.7	4.3	2.59	1.15
	-22	3.984	6.6	3.7	1.76	0.989
	-32	4.149	4.3	3.3	1.15	0.882
	-42	4.329	3.0	2.2	0.802	0.588
	-46	4.464	2.4		0.642	
4.887	38	3.215	20.5		4.12	
	24	3.367	25.9	6.3	5.20	1.27
	19	3.425	23.9	7.8	4.80	1.57
	-18	3.922	10.2	6.0	2.05	1.21
	-29	4.098	6.6	4.9	1.33	0.984
	-38	4.255	4.3	3.3	0.864	0.663
	-45	4.386	3.8	3.2	0.763	0.643
	-55	4.587	3.4	2.5	0.683	0.502
	-63	4.762	3.6	2.7	0.723	0.542
	-73	5.000	3.8	3.1	0.763	0.623

TABLE 13

Proton Chemical Shifts for $FePorClO_4$ in Methanol (60 MHz)

10^2 x complex concn molal	t, °C	$10^3/T$ $°K^{-1}$	shift, obsd, Hz		$(\Delta\omega_{obsd}/P_M) \times 10^{-4}$, rad sec^{-1}	
			-OH	$-CH_3$	-OH	$-CH_3$
3.449	30	3.300	7.5	5.5	4.27	3.13
	20	3.413	4.2	5.3	2.39	3.02
	10	3.534	3.1	4.0	1.76	2.28
	0	3.663	3.5	2.8	1.99	1.59
	40	3.195	12.3	6.7	7.00	3.81
	50	3.096	12.0	6.9	6.83	3.93
	60	3.003	11.8	6.5	6.72	3.70
	64	2.967	12.0	6.3	6.83	3.57
3.672	- 2	3.690		3.3		1.77
	-12	3.831		1.7		0.909
	-22	3.984		1.1		0.588
	-32	4.149		0.6		0.321
	-42	4.329		0.0		0.00
	-46	4.464		0.0		0.00
4.887	38	3.215	11.5		4.621	
	24	3.367	8.5	9.0	3.42	3.62
	19	3.425	7.0	8.0	2.81	3.21
	-18	3.922	3.5	3.0	1.41	1.21
	-29	4.098	2.0	1.5	0.804	0.603

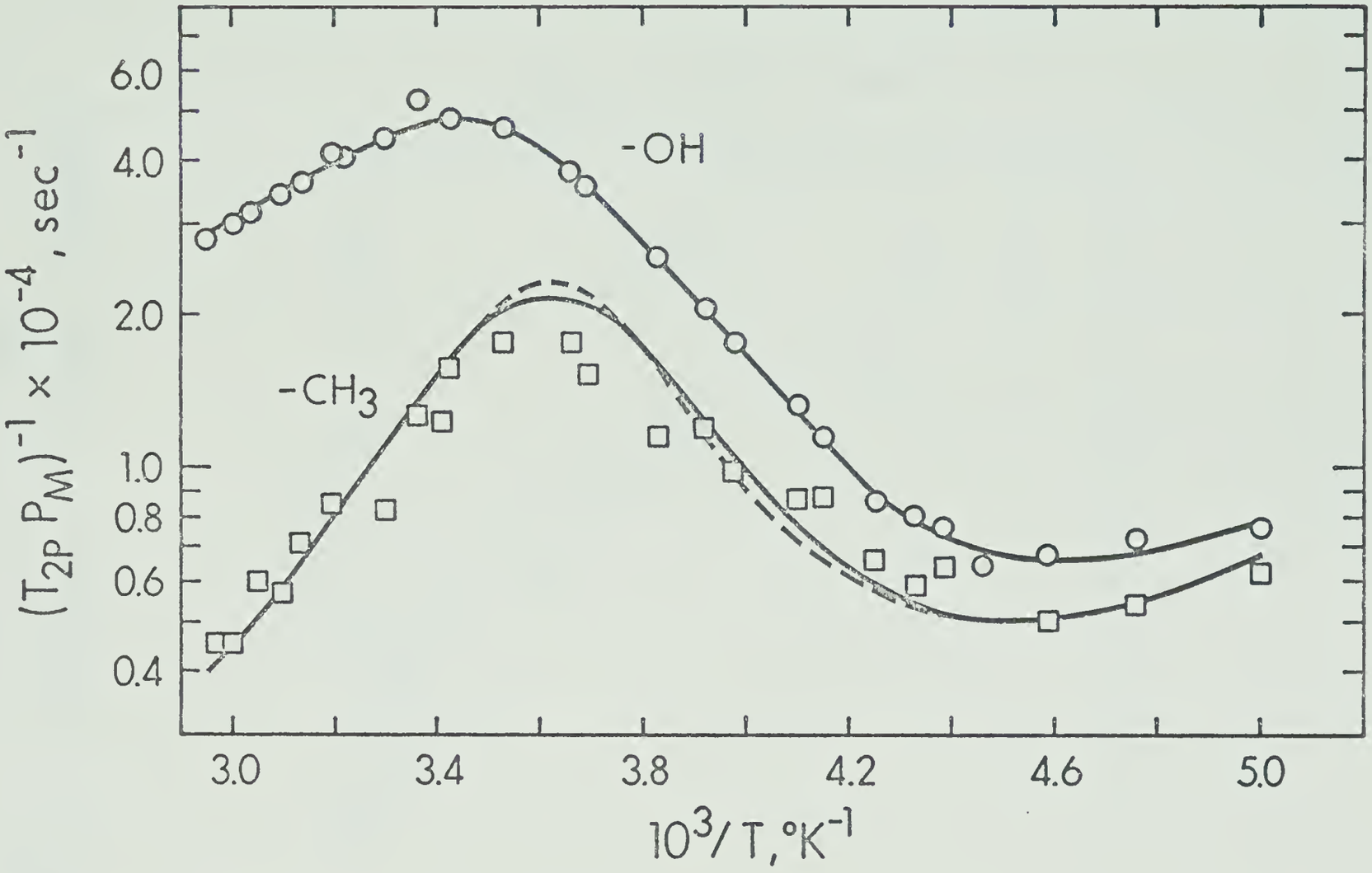

FIGURE 7. Temperature dependence of $-\log(T_{2P}P_M)$ for solutions of $FePor^+$ in methanol. Smooth curves are calculated from fits E and G and the dashed curve from fit H (Table 14).

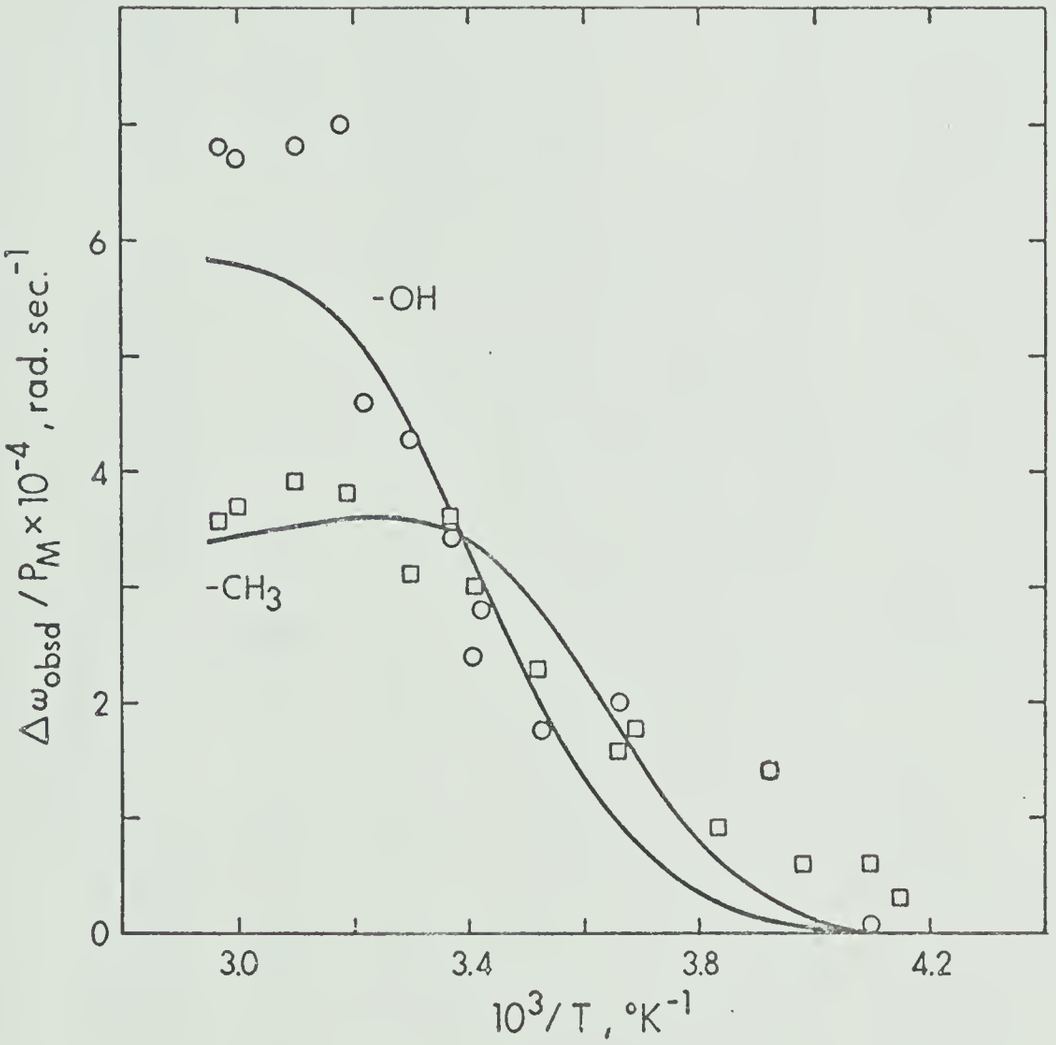

FIGURE 8: Temperature dependence of $\Delta\omega_{obsd}/P_M$ for solutions of $FePor^+$ in methanol. Smooth curves are calculated from fits J and L (Table 14).

TABLE 14

Least-squares Best-fit Parameters for $FePorClO_4$ in Methanol

	$(T_{2P}P_M)^{-1}$ Data								$\Delta\omega$ Data			
	OH Proton					CH_3 Protons			OH Proton		CH_3 Protons	
	A	B	C	D	E	F	G	H	I	J	K	L
$\Delta H^{\ddagger}$, kcal mol^{-1}	7.18	6.25	9.13	7.39	7.30	12.1	8.12	8.53	(9.13)[h]	(7.39)[i]	(12.1)[j]	(8.12)[k]
$\Delta S^{\ddagger}$, cal mol^{-1} deg^{-1}	-10.4	-13.8	-2.32	-9.52	-9.91	10.3	-7.87	-6.31	-3.99	-10.2	7.25	-7.66
10^{-2} C_M, sec^{-1}	0.591	1.12	18.8	15.3	14.8	3.06	0.998	1.07	(18.8)[h]	(15.3)[i]	(3.06)[j]	(0.998)[k]
E_M, kcal mol^{-1}	4.12	(3.75)[b]	(1.88)[c]	(1.88)[c]	(1.88)[c]	(1.88)[c]	(1.88)[c]	(1.88)[c]	(1.88)[c]	(1.88)[c]	(1.88)[c]	(1.88)[c]
C_O, sec^{-1}	67.2	0.641	72.0	67.1	66.8	57.4	58.2	59.5				
E_O, kcal mol^{-1}	1.88	(3.75)[b]	(1.88)[c]	(1.88)[c]	(1.88)[c]	(1.88)[c]	(1.88)[c]	(1.88)[c]				
10^{-7} C_ω, sec^{-1}	(0.0)[a]	(0.0)[a]	(0.0)[a]	(2.05)[d]	(2.13)[e]	(0.0)[a]	(1.11)[f]	(1.16)[g]	2.05	2.13	1.11	1.16

(a) Neglecting $\Delta\omega_M^2$ terms for preliminary fit. (b) E_M set equal to E_O. (c) Fixed at E_O value obtained in fit A. (d) Fixed at value from fit I. (e) Fixed at value from fit J. (f) Fixed at value from fit K. (g) Fixed at value from fit L. (h) Fixed at value from fit C. (i) Fixed at value from fit D. (j) Fixed at value from fit F. (k) Fixed at value from fit G.

been obtained in fits F, G and H. Qualitatively, a value of $C_\omega = 9.5 \times 10^6$ radians sec^{-1} deg would result in a better fit of the maximum region of the methyl linewidth data in Figure 7. This discrepancy (a difference in methyl C_ω of 19%) may be due to the lower accuracy of the shift data of this system due to the small shifts and limited data in the higher temperature C_ω region shown in Figure 8.

The average $\Delta H^\ddagger$ and $\Delta S^\ddagger$ parameters of fits D, E, G, H, J and L are 7.84 kcal mol^{-1} and -8.58 cal mol^{-1} deg^{-1}, respectively. These values may be used to calculate an exchange rate at 25°C, τ_M^{-1}, of 1.48×10^5 sec^{-1}, using equation 19.

The average C_ω parameters for the hydroxyl and methyl protons from fits I, J and K, L are 2.09×10^7 radians sec^{-1} deg and 1.13×10^7 radians sec^{-1} deg, respectively. These give hyperfine coupling constants ($A/\hbar$) for the hydroxyl and methyl protons of $+3.78 \times 10^6$ radians sec^{-1} and $+2.05 \times 10^6$ radians sec^{-1}, respectively, based on an effective magnetic moment of 5.9 BM [33] and using equation 20. However, the "true" value of C_ω and $A/\hbar$ for the methyl protons may be somewhat lower than that stated here, for reasons given above.

5. NMR Line Broadening Study of Porphineiron(III) Perchlorate in N,N-dimethylformamide

Three sample solutions were prepared from the por-

phineiron(III) chlorde (Mad River Chemical Co). As in previous studies, the perchlorate $FePor^{+}ClO_4^{-}$ was generated *in situ* as outlined in Chapter II. Methyl shift and linewidth data was obtained by the Lorentzian curve analysis described in previous DMF exchange studies in this thesis.

Line broadening and shift results are presented in Tables 15 and 16 and shown in Figures 9 and 10, respectively. Figure 9 shows that the formyl proton line broadening data for this system has a poorly defined τ_M^{-1} controlled region from $10^3/T = 4.2$ to 4.4 $°K^{-1}$ (-35 to -45°C). The methyl proton data is unfortunately limited by the low temperature coalescence of the *cis* and *trans* methyl resonances, which prevents curve analysis below $10^3/T = 4.4$ $°K^{-1}$ (-45°C). The methyl data do not appear to show a τ_M^{-1} controlled region at all.

The chemical shift data is of low accuracy due to the small size of the observed shifts. In particular, the methyl shifts are very small and cannot be relied on to give any quantitative parameters.

The formyl proton linewidth data were analysed using equation 17 and the temperature dependent equations (equations 19, 21, 32 and 36). The result of the non-linear least-squares computer fit is shown in Table 17. The outer-sphere relaxation "activation energy", E_O, was fixed at 2.66 kcal mol^{-1} as found for the $Fe(DMF)_6^{3+}$ -

TABLE 15

Proton Line Broadening for $FePorClO_4$ in N,N-dimethylformamide (60 MHz)

10^2 x complex concn molal	t, °C	$10^3/T$, $°K^{-1}$	$\Delta\nu_{obsd}$ -CH Hz	$\Delta\nu_{obsd}$ $-CH_3$(cis), Hz	$\Delta\nu_{obsd}$ $-CH_3$(trans) Hz	$10^{-4} \times (T_{2P}P_M)^{-1}$ -CH sec^{-1}	$-CH_3$(cis) sec^{-1}	$-CH_3$(trans) sec^{-1}
5.617	80	2.833	9.9			0.758		
	70	2.915	10.0	3.12	2.89	0.765	0.239	0.221
	60	3.003	10.6	3.46	2.39	0.811	0.265	0.183
	50	3.096	10.7	2.81	3.62	0.818	0.215	0.277
	40	3.195	11.3			0.865		
	-20	3.984	25.6			1.96		
	-10	3.802	22.0	8.83	9.83	1.68	0.676	0.752
	0	3.663	19.3			1.48		
	10	3.534	16.7	5.71	6.13	1.28	0.437	0.469
	20	3.413	14.5	4.36	5.23	1.11	0.334	0.400
	30	3.300	12.9			0.987		
	40	3.195	11.9			0.910		
4.719	40	3.195	10.8			0.984		
	33	3.268	11.4			1.04		
	- 5	3.731	16.5	3.41	7.32	1.50	0.311	0.667
	-15	3.876	19.3	4.95	8.07	1.76	0.451	0.735
	-30	4.115	23.8	6.37	9.38	2.17	0.580	0.854
	-40	4.292	23.9	10.76	13.50	2.18	0.980	1.23
	-50	4.484	24.4			2.22		

(continued.....)

TABLE 15 (continued)

4.719	-64	4.785	33.5			3.05		
	-62	4.739	31.5			2.87		
	-60	4.695	28.5			2.60		
	-55	4.587	26.0			2.37		
	-45	4.386	23.4	13.50	14.38	2.13	1.23	1.31
	-35	4.202	24.9			2.27		
	-20	4.032	22.3			2.03		
3.087	40	3.195	5.8			0.835		

TABLE 16

Proton Chemical Shifts for $FePorClO_4$ in N,N-dimethylformamide (60 MHz)

10^2 x complex concn, molal	t, °C	$10^3/T$, $°K^{-1}$	$\Delta\omega_{obsd}$ -CH Hz	$\Delta\omega_{obsd}$ $-CH_3$(cis) Hz	$\Delta\omega_{obsd}$ $-CH_3$(trans) Hz	10^{-4} x $(\Delta\omega_{obsd}/P_M)$ -CH	$-CH_3$(cis) $rad\ sec^{-1}$	$-CH_3$(trans)
5.617	80	2.833	9.4	5.04	4.00	1.44	0.771	0.612
	70	2.915	9.4	5.20	3.50	1.44	0.796	0.536
	60	3.003	9.4	5.40	3.50	1.44	0.826	0.536
	50	3.096	10.9	4.50	2.80	1.67	0.689	0.429
4.719	40	3.195	10.8			1.97		
	33	3.268	8.0			1.46		
	-5	3.731	12.1	4.63	2.05	2.20	0.843	0.373
	-15	3.876	11.5	5.08	2.56	2.10	0.925	0.466
	-30	4.115	9.8	5.11	2.09	1.79	0.931	0.381
	-40	4.292	6.8	2.83	3.50	1.24	0.519	0.637
	-50	4.484	7.3			1.33		
	-45	4.386	8.6	5.87	3.76	1.57	1.07	0.685
	-35	4.202	8.6	9.22	3.06	1.57	1.68	0.558
	-20	4.032	12.5	8.23	4.80	2.28	1.50	0.874

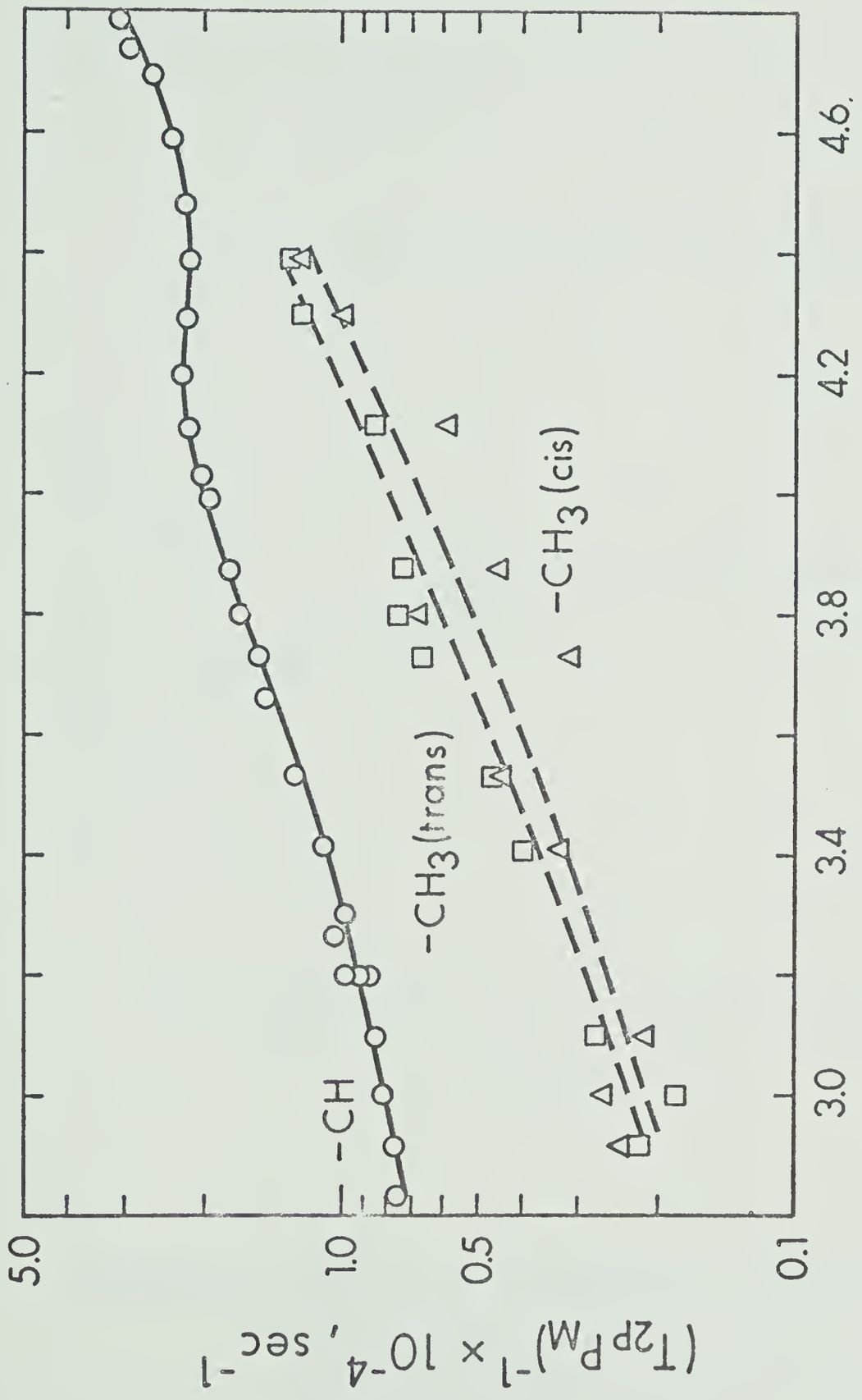

FIGURE 9: Temperature dependence of $-\log(T_{2P}P_M)$ for solutions of $FePor^+$ in N,N-dimethylformamide. Smooth curve for the CH proton is calculated from Table 17.

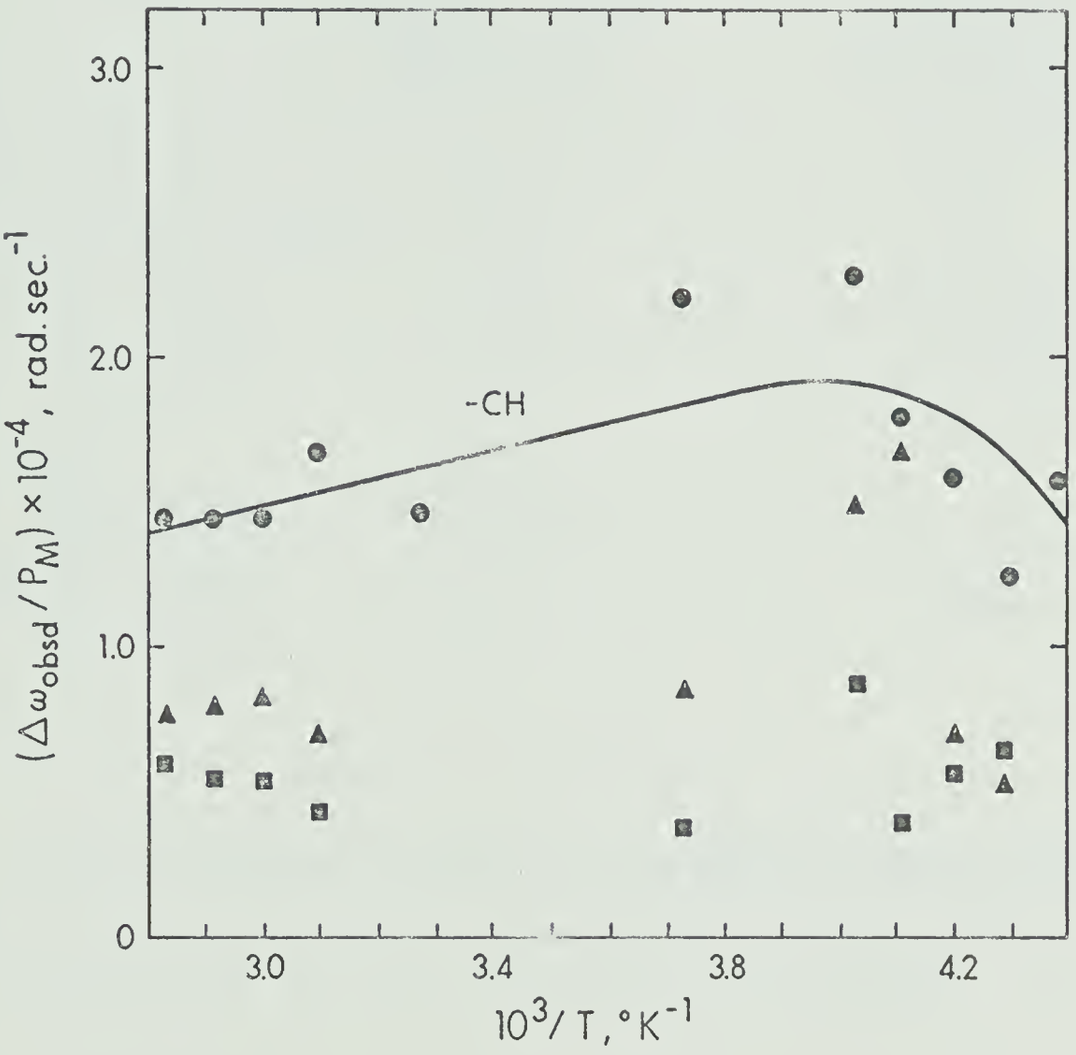

FIGURE 10: Temperature dependence of $\Delta\omega_{obsd}/P_M$ for solutions of $FePor^+$ in N,N-dimethylformamide. Smooth curve for the CH proton is calculated from Table 17. Data for cis CH_3 (▲) and trans CH_3 (■) also shown.

TABLE 17

Least-squares Best-fit Parameters for $FePorClO_4$ in N,N-dimethylformamide

	$(T_{2P}P_M)^{-1}$ Data -CH proton	Δω Data -CH proton
$\Delta H^{\ddagger}$, kcal mol^{-1}	9.01	(9.01)[b]
$\Delta S^{\ddagger}$, cal mol^{-1} deg^{-1}	-1.32	3.12
10^{-3} C_M, sec^{-1}	2.22	(2.22)[b]
E_M, kcal mol^{-1}	0.591	(0.591)[b]
C_O, sec^{-1}	47.5	-
E_O, kcal mol^{-1}	(2.66)[a]	-
10^{-6} C_ω, sec^{-1}	4.43	4.95

[a] Fixed at value obtained for $Fe(DMF)_6^{3+}$/DMF system

[b] Constrained at values indicated by $(T_{2P}P_M)^{-1}$ fit.

DMF system since only a limited outer-sphere relaxation region could be observed. The best-fit parameters shown in Table 17 were used to draw the curve in Figure 9 and adequately account for the observations. There is fairly reasonable agreement with the shift data, considering the low accuracy of the latter.

Computer analysis of the incomplete methyl data would require many assumed parameter values, hence the data has simply been analysed in a qualitative manner by assigning values to parameters which reasonably reproduce the data.

Table 18 was computed using equation 17 substituted with the temperature dependence equations. The dashed curves in Figure 9 have been drawn using these calculated values.

The cis-methyl $(T_{2P}P_M)^{-1}$ values were calculated with: $C_M = 3 \times 10^2$ sec^{-1}, $E_M = 0.591$ kcal mol^{-1}, $\Delta H^{\ddagger} = 9.01$ kcal mol^{-1}, $\Delta S^{\ddagger} = -1.32$ cal deg^{-1} mol^{-1}, $C_\omega = 1 \times 10^6$ radians sec^{-1} deg, $C_O = 24.89$ sec^{-1} and $E_O = 2.66$ kcal mol^{-1}. The trans-methyl $(T_{2P}P_M)^{-1}$ values were calculated with: $C_M = 2 \times 10^2$ sec^{-1}, $E_M = 0.591$ kcal mol^{-1}, $\Delta H^{\ddagger} = 9.01$ kcal mol^{-1}, $\Delta S^{\ddagger} = -1.32$ cal deg^{-1} mol^{-1}, $C_\omega = 8 \times 10^5$ radians sec^{-1} deg, $C_O = 32.97$ sec^{-1} and $E_O = 2.66$ kcal mol^{-1}. The C_O values were estimated in the same way as the $FeTPP^+$ - DMF system methyl data (see section 2).

The above parameters predict $\Delta\omega_{obsd}/P_M$ values lower

TABLE 18

Calculated and Observed Line Broadening Data for the Methyl Protons of DMF Solutions of $FePor^+$

t, °C	$10^3/T$, $°K^{-1}$	Cis-methyl $(T_{2P}P_M)^{-1} \times 10^{-3}$, sec^{-1}		Trans-methyl $(T_{2P}P_M)^{-1} \times 10^{-3}$, sec^{-1}	
		Obsd.	Calc.	Obsd.	Calc.
60	3.003	2.65	2.12	1.83	2.33
50	3.096	2.15	2.33	2.77	2.58
20	3.413	3.34	3.25	4.00	3.74
10	3.534	4.37	3.71	4.69	4.33
-15	3.876	4.51	5.62	7.35	6.68
-30	4.115	5.80	7.81	8.54	9.27
-40	4.292	9.80	9.99	12.3	11.9
-45	4.386	12.3	11.2	13.1	13.5

than those found experimentally and shown in Table 16. However, the precision of the $\Delta\omega_{obsd}$ observations, after Lorentzian curve analysis, is of the order of ± 2 Hz. The parameters used above in the methyl $(T_{2P}P_M)^{-1}$ analysis are in agreement with the $\Delta\omega_{obsd}/P_M$ data within this error range.

The $\Delta H^{\ddagger}$ value of 9.01 kcal mol^{-1} and $\Delta S^{\ddagger}$ value of -1.32 cal deg^{-1} mol^{-1} give an exchange rate at 25°C, τ_M^{-1}, of 7.96×10^5 sec^{-1}. It must be emphasized that the accuracy of the exchange parameters obtained for this system is very low because of the ill-defined τ_M^{-1} exchange controlled region observed in the linewidth data.

D I S C U S S I O N

CHAPTER IV

1. Kinetic Results

(a) DMF exchange from $Fe(DMF)_6^{3+}$.

The kinetic results from this study are shown in Table 19. The observations reported here are qualitatively similar to those found previously by Breivogel.[59] However, the $(T_{2P}P_M)^{-1}$ values shown in Figure 2 are consistently smaller than those from the earlier work, by as much as a factor of 2-3 in the low-temperature outer-sphere region. The differences in kinetic parameters are due largely to the differences in the correction for the outer-sphere effects. The outer-sphere activation energy (E_o) of 3.5 kcal mol^{-1} found by Breivogel is higher than values which have been found for several systems reported in references 1,57,58,60, and is also higher than the activation energy for viscosity of DMF (~2.8 kcal mol^{-1}).[61]

The very negative $\Delta S^{\ddagger}$ for DMF exchange with $Fe(DMF)_6^{3+}$ may indicate an associative type mechanism for this reaction. Fiat and Connick [20] have proposed that the negative $\Delta S^{\ddagger}$ of -22 cal mol^{-1} deg^{-1} for water exchange on gallium(III), compared to +28 cal mol^{-1} deg^{-1} for the analogous aluminum(III) system, is evidence for an associative mechanism with gallium(III). The ionic radius of iron(III) (0.64 Å) is close to that of gallium(III) (0.62 Å),

TABLE 19

Kinetic Parameters for Solvent Exchange of Iron and Iron(III) Porphyrin Systems

Complex/Solvent	τ_M^{-1} (25°C) sec^{-1}	$\Delta H^{\ddagger}$ kcal mol^{-1}	$\Delta S^{\ddagger}$ cal mol^{-1} deg^{-1}	Reference
$Fe(DMF)_6^{3+}/DMF$	61	10.1 ± 1	-16.5 ± 3	a
	28	12.5 ± 1.5	-10 ± 5	59
$Fe(DMF)_6^{2+}/DMF$	1.6×10^6	11.7	9.12	62
$FeTPP(DMF)^{+}/DMF$	5.4×10^6	9.4 ± 0.4	3.8 ± 0.7	a
$FePor(DMF)^{+}/DMF$	8.0×10^5	9.01	-1.32	a
$Fe(MeOH)_6^{3+}/MeOH$	5.1×10^3	10.1	-8	59
	2.4×10^3	10.7	-7	59
$Fe(MeOH)_6^{2+}/MeOH$	4.5×10^4	12.0	3	63
$FeTPP(MeOH)^{+}/MeOH$	3.0×10^6	11.3	9.0	a
$FePor(MeOH)^{+}/MeOH$	1.5×10^5	7.84	-8.58	a
$Fe(C_2H_5OH)_6^{3+}$	2.1×10^4	6.2 ± 1.5	−18 ± 5	59
$HEMIN(C_2H_5OH)/C_2H_5OH + H_2O$	3.6×10^6	6.2 ± 1.0	−7.7 ± 5	2,(b)
$Fe(H_2O)_6^{2+}/H_2O$	3.1×10^6	7.7	-3.0	41

(a) This work

(b) Values recalculated assuming a solvation number of one.

and a common associative mechanism seems plausible on this basis. Although the steric bulk of DMF might be expected to favor a dissociative mechanism, DMF is an essentially planar molecule and a seven coordinate intermediate is possible.

The solvent exchange kinetics of iron(III) in dimethylsulfoxide (DMSO), ethanol and methanol have been studied previously. All of these systems have negative $\Delta S^{\ddagger}$ values providing some indication that an associative mechanism may be operative more generally for hexasolvated iron(III) systems. In the study of the DMSO system Langford and Chung [64] took the negative $\Delta S^{\ddagger}$ to be typical of a dissociative mechanism because they compared it to an incorrect value of -16 cal mol^{-1} deg^{-1} for nickel(II)-DMSO exchange. The latter value is 1.2 cal mol^{-1} deg^{-1} from the most recent study.[65]

Unfortunately, despite early studies by Connick and recent work by Hunt, there is no reliable exchange rate for the iron(III)-water system. All studies have encountered complications due to hydrolysis and slow polymerization of aqueous iron(III).

It is surprising that Brievogel did not have similar trouble with iron(III) in ethanol and methanol. That Brievogel may not have noted chemical changes in his iron(III)-alcohol solutions is implied also from his study of the iron(III)-acetonitrile system which Kratochvil and

Long [66] have shown to be highly unstable.

The fact that the exchange rates for ethanol and methanol are ~10^3 and ~10^2 times respectively faster than the DMF exchange rate on iron(III) seems unusual. At least for all the dipositive ions studied so far (cobalt, nickel, manganese, iron) DMF exchanges faster than methanol at 25°. Breivogel argues that the alcohols exchange faster because steric effects favor a dissociative mechanism, but this does not seem consistent with the negative $\Delta S^{\ddagger}$ values. These steric arguments also are not consistent with the fact that methanol exchange on magnesium(II) is slower than water exchange, yet the crystal radius of Mg^{2+} is only 0.02 Å larger than that of Fe^{3+}.

A comparison of the solvent exchange rates on magnesium(II) and iron(III) would be of considerable interest. Neither metal ion should have any crystal field contributions and they have very similar ionic radii, so that kinetic differences would be solely due to the charge difference. Unfortunately the only systems which are directly comparable are methanol and ethanol and the results for iron(III) are in doubt as noted above. However, results for magnesium are similar to those for nickel(II) with positive $\Delta S^{\ddagger}$ values and it seems that the increase in charge from magnesium(II) to iron(III) may have brought about a change from a dissociative to an associative type mechanism.

(b) Solvent exchange from iron(III) porphyrin systems

A qualitative comparison of the exchange rates of the iron(III) hexasolvated and porphyrin systems shows a rate enhancement of 10^3 to 10^4 for the porphyrins. The factor does not appear so large for methanol, but this may be due to problems with the hexasolvated system noted above. Previous studies of ligand substitution on cobalt(III) and chromium(III) porphyrins [67,3,68] have also shown them to react faster than the simpler complexes, such as $(NH_3)_5CoOH_2^{3+}$ and $(NH_3)_5CrOH_2^{3+}$, by about the same factor.

Several reasons for this enhancement have been proposed. Fleischer suggested that it might be due to the metal ion being displaced above the porphyrin plane so that the complexes are not structurally analogous to octahedral complexes. Certainly this feature is present with high spin iron(III) porphyrins, but a number of recent studies show that cobalt(III) is normally in the porphyrin plane with two symmetrically bonded axial ligands.[69,70,71] Therefore distortion from C_{4v} symmetry cannot be invoked to account for the reactivity of the cobalt(III) porphyrins.

It has been noted by Hoard [72] for iron(III) and by Ibers [69] for cobalt(III) porphyrins that the axial ligand-metal bond lengths are quite similar to those in simple complex ions of the same metal ions. This is also consistent with the observations of both Fleischer [67] and Pasternack [68] that the pK_a of a water molecule coordinated to either

a cobalt(III) or chromium(III) porphyrin is quite similar to the pK_a of coordinated water in the corresponding $(NH_3)_5MOH_2^{3+}$ complex.

The conclusion from the above observations is that the kinetic lability of the porphyrin systems is not due to weakening of the metal-axial ligand bond. Therefore, it seems that added stabilization of the transition state causes the faster substitution reactions of the porphyrins.

A recent study on cobalt(III) Schiff base complexes[73] has shown that the hydrolytic reactivity is greatly influenced by the number of azomethine (N=C) nitrogens bonded to the metal. The halide complex hydrolysis rate increases by $\sim 10^4$ as the number of such linkages increases from zero to four.[73] The pyrrole nitrogens in the porphyrin are also part of an N=C bond and this may be the source of the high reactivity of the porphyrin. It may be noted that a nickel (II) Schiff base complex[58], $Ni(TAAB)(DMF)_2^{2+}$ with four azomethine nitrogen to metal bonds exchanges DMF twenty times faster than $Ni(DMF)_6^{2+}$. However, the three coordinate chelate analogue of TAAB, $Ni(TRI)(DMF)_3^{2+}$ exchanges[58] DMF six times slower than $Ni(DMF)_6^{2+}$. Thus the increased reactivity seems to be associated with azomethine groups in a square planar arrangement around the metal ion and is not simply due to electron donation or withdrawal from the metal ion.

These observations point to some stabilization of the

transition state due to π bonding between the metal and the N=C system, or with the full π (or π*) system in the porphyrins. There are various ways in which this may operate depending on whether the metal is a π acceptor or donor in the ground state, and whether the substitution mechanism is associative or dissociative.

For the porphyrin systems studied here the solvent exchange rate at 25° is larger for FeTPP (see Table 19) with a larger $\Delta H^{\ddagger}$ being compensated by a more positive $\Delta S^{\ddagger}$. It also appears that the magnitude of the difference in the two systems depends on the axial ligand, which is also the solvent in these cases.

The activation parameters, especially in methanol seem to indicate a more dissociative mechanism for FeTPP and a more associative one for FePor, the opposite of what would be predicted from the fact that Por is a better σ donor ligand. However, this should not be too surprising in view of the arguments advanced earlier that π interactions in the transition state may be the more important factor. It seems pointless to speculate further because it is not even clear whether the porphyrin is a π donor or acceptor relative to high spin iron(III). Molecular orbital calculations [29] indicate that iron(III) is a net π acceptor, while nmr results have been interpreted to indicate that it is a donor of π electron density.[74]

Finally an alternative mechanism for solvent exchange

should be mentioned. For these iron(III) porphyrins the metal atom sits above the porphyrin plane. Solvent exchange would result if the iron atom moved down through the plane to a position on the other side of the porphyrin. Such an "inversion" has been observed in para CH_3TPPFeCl [75] (with a p-tolyl group instead of phenyl in TPP) however the rate constant of 4.5×10^2 sec^{-1} at 25° seems much too small to make this a likely path for solvent exchange in the systems studied here.

2. Activation Enthalpy - Solvent Coordinating Power Correlations.

Enthalpies of adduct formation have been successfully correlated to two parameters assigned to the donor and acceptor molecules respectively.[76,77] Drago and Wayland proposed a double-scale equation,

$$-\Delta H = E_A E_B + C_A C_B \qquad (41)$$

where subscripts A and B indicate acceptor and donor respectively, while E and C are two empirically determined parameters for each. The E and C were interpreted as being related to the electrostatic and covalent bond forming abilities of the molecules, normalized to $E_A = C_A = 1$ for iodine.

In a search for a measure of basicity which might be used to correlate kinetic results the product $C_B E_B$ has

been chosen.[57] It was found empirically that for a particular metal ion $\Delta H^{\ddagger}$ values for solvent exchange reactions may be correlated with $C_B E_B$ values for the solvents. Such correlations contain both a direct and inverse relationship with respect to $C_B E_B$.

The correlation given in reference 57 is:

$$\Delta H^{\ddagger} = \frac{X}{C_B E_B} (\log C_B E_B + Y) \qquad (42)$$

where X and Y are empirically determined parameters characteristic of a particular metal ion.

An alternative equation has been proposed by Hoffmann[78]:

$$\Delta H^{\ddagger} = AC_B E_B \, \mathrm{Exp}(-BC_B E_B) \qquad (43)$$

where A and B are empirically determined.

Equations 42 and 43 were used with an iterative least-squares computer program[79] to determine values for X, Y and A, B for various metal ions. The results are shown as Fits 1 in Tables 20 and 21 and utilize the $\Delta H^{\ddagger}_{obs}$ data shown in Table 19. The following $C_B E_B$ values from reference 77 were used; NH_3, 4.71; DMSO, 3.82; DMF, 3.05; and CH_3CN, 1.19.

A problem in this work has been the absence of C_B, E_B values for water and methanol. Fits 1 in Tables 20 and 21 were used to obtain self-consistent $C_B E_B$ values for water or

TABLE 20

Least Squares Fitting Results for X, Y and C_BE_B Values

Fit Number		Metal Ion Ni^{2+}	Co^{2+}	Mn^{2+}	Fe^{2+}	$NiCR^{2+}$	Fe^{3+}	C_BE_B H_2O	MeOH
1	X[a]	59.7	55.4	46.9				1.07[b]	1.29[b]
	Y[a]	0.234	0.129	0.108					
2	X	62.5	65.5	43.2	87.6	48.9	50.2	0.987[b]	1.15[b]
	Y	0.206	0.143	0.129	0.620	0.116	0.148		
3	X	61.0	62.4	41.7	68.9	44.3	47.7	4.96[c]	3.14[c]
	Y	0.233	0.170	0.152	0.129	0.153	0.183		
4	X	65.0	66.1	42.2	52.8	47.3	77.9	4.72[c]	2.66[c]
	Y	0.208	0.131	0.124	0.146	0.103	-0.0916		
5	X	63.1	64.8	41.7	49.7	45.9	71.8	4.50[c]	2.48[c]
	Y	0.221	0.135	0.121	0.162	0.109	-0.0536		

[a] Values obtained omitting H_2O, MeOH data.

[b] Fit obtained with primary guess 1.0

[c] Fit obtained with primary guess 4.0

TABLE 21

Least Squares Fitting Results for A, B and C_BE_B Values

Fit Number		Metal ion						C_BE_B [b]	
		Ni^{2+}	Co^{2+}	Mn^{2+}	Fe^{2+}	$NiCR^{2+}$	Fe^{3+}	H_2O	MeOH
1	A[a]	23.6	15.3	9.12				3.93	2.77
	B[a]	0.513	0.402	0.362					
2	A	23.7	15.7	7.65	15.6	10.52	8.56	4.03	2.29
	B	0.510	0.420	0.340	0.501	0.427	0.311		
3	A	23.0	15.7	7.27	15.8	10.6	9.51	Standard error increased	
	B	0.502	0.419	0.321	0.511	0.430	0.341		
4	A	23.5	15.3	9.38	12.6	8.85	8.62		2.8[c]
	B	0.508	0.401	0.363	0.378	0.344	0.313		

a. Values obtained omitting H_2O, MeOH data

b. Fits obtained with primary guess 4.0

c. Value used in fitting the $NiCR^{2+}$ and Fe^{3+} data only.

methanol by using an iterative least-squares computer program to fit the data to the equation

$$F = \frac{1}{C_B E_B} \left\{ X(1)(\log C_B E_B + Y(1)) + \ldots . X(n)(\log C_B E_B + Y(n)) \right\} \qquad (44)$$

The input data was arranged such that $F = \Delta H^{\ddagger}(\ell)$ with $X(\ell)$, $Y(\ell)$ and all other $X(m)$, $Y(m)$ in the computer program input data set equal to zero.

A similar procedure was followed using equation 43:

$$F = C_B E_B \left\{ A(1)\mathrm{Exp}(-B(1)C_B E_B) + \ldots A(n)\mathrm{Exp}(-B(n)C_B E_B) \right\} \qquad (45)$$

where $F = \Delta H^{\ddagger}(\ell)$ with $A(\ell)$ and $B(\ell)$, all other $A(m)$, $B(m)$ being set equal to zero.

Subsequent fits for X, Y and A, B were made utilizing methanol and water $C_B E_B$ values, each value being obtained from the previous X, Y or A, B parameters. This procedure was repeated until the standard errors on the computer fits started to increase.

Two points of convergence of the $C_B E_B$ least-squares fits could be obtained, depending on the choice of the primary guess required to begin the iterative fitting procedure. One set of values was found with input guesses around unity and another one with a value of 4.0.

The higher values for water and methanol are chemically more reasonable. Fitting to equation 44 gives values of 4.50 and 2.48 to C_BE_B for water and methanol, respectively, whereas equation 45 yields values of 4.03 and 2.29. Both correlations place H_2O between NH_3 and DMSO, and methanol between CH_3CN and DMF, in terms of coordinating power (C_BE_B).

Equation 45 was found to provide the methanol and water C_BE_B values with lower standard errors on the fits than equation 44. For this reason equation 43 may be said to provide a better correlation of $\Delta H^{\ddagger}$ to C_BE_B than equation 42.

Table 22 shows values of $\Delta H^{\ddagger}$ predicted for solvent exchange for various metal ions, using equation 43 with Table 21, fit 2, A and B parameters, C_BE_B values given in reference 77 and C_BE_B values of 4.03 and 2.29 for water and methanol respectively.

Of the 27 predicted values 21 are within $\pm$ 0.8 kcal $mole^{-1}$ of the observed values and 15 are within $\pm$ 0.5 kcal $mole^{-1}$. Since the error limits on the experimental values are probably of the order of $\pm$ 0.5 to 1 kcal $mole^{-1}$ better agreement of predicted and experimental values is not to be expected.

However, a closer analysis of the predicted values shows some anomalies. For example with manganese(II), only the water $\Delta H^{\ddagger}$ is well predicted but this is an arti-

TABLE 22

Observed and Calculated Enthalpy of Activation Data

Solvent	Metal Ion	$\Delta H^{\ddagger}_{obs}$ (kcal mol^{-1})	$\Delta H^{\ddagger}_{calc}$ [a] (kcal mol^{-1})	Reference
NH_3	Ni(II)	11	10.1	80
CH_3CN		15.0	15.4	81
CH_3CN		16.4	15.4	82
DMF		15.0	15.3	83
DMF		14.0	15.3	16
DMSO		12.1	12.9	84
DMSO		13.0	12.9	15
CH_3OH		15.8	16.9	50
H_2O		12.1	12.2	85
H_2O		13.9	12.2	86
NH_3	Co(II)	11.2	10.2	87
CH_3CN		11.4	11.3	88
DMF		13.6	13.3	58
DMSO		12.2	12.1	15
CH_3OH		13.8	13.7	50
H_2O		10.4	11.6	89
NH_3	Mn(II)	8	7.26	90
CH_3CN		7.25	6.07	91
DMF		8.9	8.27	92
CH_3OH		6.2	8.04	63
H_2O		7.85	7.83	93

(continued.....)

TABLE 22 (continued)

CH_3CN	Fe(II)	9.7	10.2	82
CH_3OH		12.0	11.3	63
H_2O		7.7	8.35	41
DMF		11.7	10.3	62
DMSO		11.7	8.79	62
DMSO	Fe(III)	10.0	9.97	64
DMF		10.1	10.1	This work
CH_3OH		10.1	9.62	63
DMF	NiCR(II)	9.5	8.72	60
H_2O		6.8	7.59	60
CH_3OH		9.4	9.06	57
CH_3CN		7.0	7.53	57

(a) Calculated using equation 43 with Table 21, fit 2, A and B parameters. Reference 77 C_BE_B values and values of 4.03 and 2.29 for water and methanol, respectively, were also used.

fact because the C_BE_B value for water was used as a variable. Furthermore, some of the apparently better experimental values, those for which a long exchange controlled region is observed, are not well predicted. Specifically these systems are nickel(II), cobalt(II) and manganese(II) in ammonia, nickel(II) in methanol and manganese(II) in acetonitrile. Finally for iron(II) in DMF and DMSO the predicted values of 10.3 and 8.8 kcal $mole^{-1}$ respectively, do not agree with the recently determined value of 11.7 kcal $mole^{-1}$ in both systems.[62]

Subsequent analysis has indicated that these problems arise largely because some of the water exchange $\Delta H^{\ddagger}$ values are not consistent with eq. 43, especially in the case of manganese(II) and iron(II). With the new data available for iron(II) in DMF and DMSO a simple least squares fit to eq. 43 can be done for nickel(II), cobalt(II), manganese(II) and iron(II), excluding results for water and methanol. The resulting A and B parameters, given as fit 4 in Table 21, predict $\Delta H^{\ddagger}$ values within $\pm$ 0.5 kcal $mole^{-1}$ for nickel(II), cobalt(II), iron(II) and manganese(II), except for a difference of 0.9 kcal $mole^{-1}$ for the nickel(II)-NH_3 system. In addition a C_BE_B value of 2.8 for methanol predicts the $\Delta H^{\ddagger}$ for methanol exchange, except for manganese(II), and the C_BE_B value gives a good fit for the $NiCR^{2+}$ and iron(III) systems. This analysis fits 21 out of 23 $\Delta H^{\ddagger}$ values, the two exceptions being nickel(II)-NH_3 and manganese(II)-CH_3OH.

However, the water exchange results have not been considered. These $\Delta H^{\ddagger}$ values are reasonably ($\pm$ 0.8 kcal $mole^{-1}$) accounted for if $C_B E_B \approx 1$ for H_2O, except for the manganese-(II) value. But such a low $C_B E_B$ value does not seem consistent with the expected basicity of water as already noted. If an intuitively more reasonable $C_B E_B$ of 3.5 - 4 is chosen, then only nickel(II) and manganese(II) give reasonable predicted $\Delta H^{\ddagger}$ values. These difficulties with water may not be a failure of the correlation because there are ambiguities in the interpretation of the data for manganese(II) and $NiCR^{2+}$, and iron(II) was studied over ten years ago in the pioneer study in this field.

In any case, to return to the porphyrin systems, it is not possible to use the correlation to calculate $\Delta H^{\ddagger}$ for water exchange. In retrospect, if such a calculation were to be made it would be best to extrapolate from two solvents of widely differing $C_B E_B$ values. Thus DMF and methanol are not particularly suitable and future studies in acetonitrile could prove more useful in this respect.

REFERENCES

1. L. L. Rusnak and R. B. Jordan, Inorg. Chem., 11, 196 (1972).
2. N. S. Angerman, B. B. Hasinoff, H. B. Dunford, and R. B. Jordan, Can. J. Chem., 47, 3217 (1969).
3. E. B. Fleischer, S. Jacobs, and L. Mestichelli, J. Amer. Chem. Soc., 90, 2527 (1968).
4. M. Weissbluth, "Structure and Bonding", Vol. 2, page 1. Springer 1967.
5. K. Wüthrich, ibid., Vol. 8, page 53.
6. (a) J. E. Falk, "Porphyrins and Metalloporphyrins", Elsevier Publishing Co., New York, N.Y., 1964.
   (b) A. D. Adler (Editor), Ann. N.Y. Acad. Sci., Vol. 206, (1973).
7. L. J. Boucher, Coordin. Chem. Rev., 6, 247 (1971).
8. F. Basolo and R. G. Pearson, "Mechanisms of Inorganic Reactions", Chap. 3, page 124. John Wiley and Sons Inc.
9. C. H. Langford and H. B. Gray, "Ligand Substitution Processes", W. A. Benjamin, Inc.
10. T. R. Stengle and C. H. Langford, Coordin. Chem. Rev., 2, 349 (1967).
11. D. J. Hewkin and R. H. Prince, ibid., 5, 45 (1970).
12. J. P. Hunt, ibid., 7, 1 (1971).
13. R. A. Dwek, Advan. Mol. Relaxation Processes, 4, 53 (1972).

14. H. G. Hertz, "Progress in NMR Spectroscopy", Vol. 3, page 159. Edited by J. W. Emsley, J. Feeney and L. H. Sutcliffe. Pergamon Press, (1967).

15. L. S. Frankel, Inorg. Chem., 10, 814 (1971).

16. L. S. Frankel, ibid., 10, 2360 (1971).

17. G. S. Vigee and P. Ng, J. Inorg. Nucl. Chem., 33, 2477 (1971).

18. W. K. Kruse and D. Thusius, Inorg. Chem., 7, 464 (1968).

19. B. R. Baker, N. Sutin and T. J. Welch, ibid.,6, 1948 (1967).

20. D. Fiat and R. E. Connick, J. Amer. Chem. Soc., 90, 608 (1968).

21. C. H. Langford and F. M. Chung, Can. J. Chem., 48, 2969 (1970).

22. E. B. Fleischer, Accounts of Chem. Res., 3, 105 (1970).

23. J. L. Hoard, "Structural Chemistry and Molecular Biology", page 573. A. Rich and N. Davidson, Editors.

24. P. S. Braterman, R. C. Davies and R. J. P. Williams, "Advances in Chemical Physics", Vol. VII, page 359.

25. P. Hambright, Coordin. Chem. Rev., 6, 247 (1971).

26. J. L. Hoard, G. H. Cohen and M. D. Glick, J. Amer. Chem. Soc., 89, 1992 (1967).

27. D. F. Koenig, Acta. Cryst., 18, 663 (1965).

28. J. L. Hoard, M. J. Hamor, T. A. Hamor and W. S. Caughey, J. Amer. Chem. Soc., 87, 2312 (1965).

29. M. Zerner, M. Gouterman and H. Kobayashi, Theoret. Chim. Acta., 6, 363 (1966).

30. M. Zerner and M. Gouterman, Theoret. Chim. Acta., 4, 44 (1966).

31. M. Gouterman, J. Mol. Spec., 6, 138 (1961).

32. L. Edwards, D. H. Dolphin and M. Gouterman, J. Mol. Spec., 35, 90 (1970).

33. C. Maricondi, W. Swift and D. K. Straub, J. Amer. Chem. Soc., 91, 5205 (1969).

34. G. H. Loew, J. Mag. Res., 6, 408 (1972).

35. A. Wolberg and J. Manassen, J. Amer. Chem. Soc., 92, 2982 (1970).

36. P. L. Richards, W. S. Caughey, H. Eberspaecher, G. Feher and M. Malley, J. Chem. Phys., 47, 1187 (1967).

37. G. C. Brackett, P. L. Richards, and W. S. Caughey, J. Chem. Phys., 54, 4383 (1971).

38. C. P. Scholes, R. A. Isaacson and G. Feher, Biochim. Biophys. Acta., 244 , 206 (1971).

39. G. N. La Mar and F. Ann Walker, J. Amer. Chem. Soc., 95, 6950 (1973).

40. J. A. Pople, W. G. Schneider and H. J. Bernstein, "High-Resolution Nuclear Magnetic Resonance", Chapter 3. McGraw-Hill Book Co.

41. T. J. Swift and R. E. Connick, J. Chem. Phys., 37, 307 (1962).

42. J. S. Leigh Jr., J. Mag. Res., 4, 308 (1971).

43. H. M. McConnell, J. Chem. Phys., 28, 430 (1958).

44. N. Bloembergen, J. Chem. Phys., 27, 595 (1957).

45. I. Solomon, Phys. Rev., 99, 559 (1955).

46. N. Bloembergen, J. Chem. Phys., 27, 572 (1957).

47. R. E. Connick and D. Fiat, ibid., 44, 4103 (1966).

48. A. D. McLachlan, Proc. Roy. Soc., 280, 271 (1964).

49. M. Rubinstein, A. Baram and Z. Luz, Mol. Phys., 20, 67 (1971).

50. Z. Luz and S. Meiboom, J. Chem. Phys., 40, 2686 (1964).

51. D. Dolphin, J. Heterocyclic Chem., 7, 275 (1970).

52. A. D. Adler, F. R. Longo, F. Kampas and J. Kim, J. Inorg. Nucl. Chem., 32, 2443 (1970).

53. G. D. Dorough, J. R. Miller and F. M. Huennekens, J. Amer. Chem. Soc., 73, 4315 (1951).

54. E. B. Fleischer, J. M. Palmer, T. S. Srivastava and A. Chatterjee, ibid., 93, 3162 (1971).

55. R. Sumner, Ph.D. Thesis, University of Alberta, 1971.

56. N. S. Angerman and R. B. Jordan, J. Chem. Phys., 54, 837 (1971).

57. L. L. Rusnak, Ph.D. Thesis, University of Alberta, 1971.

58. L. L. Rusnak, J. E. Letter Jr. and R. B. Jordan, Inorg. Chem., 11, 199 (1972).

59. F. W. Breivogel Jr., J. Phys. Chem., 73, 4203 (1969).

60. L. L. Rusnak and R. B. Jordan, Inorg. Chem., 10, 2686 (1971).

61. R. B. Jordan and N. S. Angerman, J. Chem. Phys., 48, 3983 (1968).

62. S. Funahashi and R. B. Jordan, unpublished results.

63. F. W. Breivogel, J. Chem. Phys., 51, 445 (1969).

64. C. H. Langford and F. M. Chung, J. Amer. Chem. Soc., 90, 4485 (1968).

65. C. Boubel and J. J. Delpuech, J. Chim. Phys., 70, 578 (1973).

66. B. Kratochvil and R. Long, Anal. Chem., 42, 43 (1970).

67. R. F. Pasternak and M. A. Cobb, Biochem. Biophys. Res. Comm., 51, 507 (1973).

68. E. B. Fleischer and M. Krishnamurthy, J. Coord. Chem., 2, 89 (1972).

69. J. W. Lauher and J. A. Ibers, J. Amer. Chem. Soc., 96, 4447 (1974).

70. W. R. Schmidt, J. A. Cunningham and J. L. Hoard, J. Amer. Chem. Soc., 95, 8289 (1973).

71. S. Risdale, J. C. Cassat and J. Steinhardt, J. Biol. Chem., 248, 771 (1973).

72. J. L. Hoard, Science, 174, 1295 (1971).

73. D. P. Rillema, J. F. Endicott and J. R. Barber, J. Amer. Chem. Soc., 85, 6987 (1973).

74. F. A. Walker and G. N. La Mar, see reference 6(b), page 328.

75. G. N. La Mar, J. Amer. Chem. Soc., 95, 1662 (1973).

76. R. S. Drago and R. B. Wayland, J. Amer. Chem. Soc., 87, 3751 (1965).

77. R. S. Drago, G. C. Vogel and T. E. Needham, J. Amer. Chem. Soc., 93, 6014 (1971).

78. Private communication.

79. "ENNLSQ", by L. L. Rines, J. A. Plambeck and D. J. Francis, Chem. Dept., University of Alberta.

80. H. M. Glaeser, G. A. Lo, H. W. Dodgen and J. P. Hunt, Inorg. Chem., 4, 206 (1965).

81. I. D. Campbell, J. P. Carver, R. A. Dwek, A. J. Nummelin and R. E. Richards, Mol. Phys., 20, 913 (1971).

82. R. J. West and S. F. Lincoln, Aust. J. Chem., 24, 1169 (1971).

83. N. A. Matwiyoff, Inorg. Chem., 5, 788 (1966).

84. N. S. Angerman and R. B. Jordan, Inorg. Chem., 8, 2579 (1969).

85. D. Rablen and G. Gordon, ibid., 8, 395 (1968).

86. J. W. Neely and R. E. Connick, J. Amer. Chem. Soc., 94, 3419 (1972), and ibid., 94, 8646 (1972).

87. R. Murray, S. F. Lincoln, H. H. Glaeser, H. W. Dodgen, and J. P. Hunt, Inorg. Chem., 8, 554 (1969).

88. R. J. West and S. F. Lincoln, ibid., 11, 1688 (1972).

89. A. M. Chmelnick and D. Fiat, J. Chem. Phys., 47, 3986 (1967).

90. M. Grant, H. W. Dodgen and J. P. Hunt, J. Amer. Chem. Soc., 91, 6318 (1969).

91. W. L. Purcell and R. S. Marianelli, Inorg. Chem., 9, 1724 (1970).

92. Tzeng-ming Chen and L. O. Morgan, J. Phys. Chem., 76, 1973 (1972).

93. M. S. Zetter, M. W. Grant, E. J. Wood, H. W. Dodgen and J. P. Hunt, Inorg. Chem., 11, 2701 (1972).